PART C

DUCTILE STRUCTURES

CHAPTER NINE

Ductile Deformation Processes

9.1 INTRODUCTION

How can a strong layer of rock permanently bend into a tight fold (Figure 9.1)? How can a material such as ice distort, while remaining a solid? Ice is a particularly instructive example of flow in crystalline solids, because it moves on human timescales. Its behavior is directly relevant to rock deformation on geologic timescales. At first one might think that solid deformation is accomplished by bending and stretching of atomic bonds in the crystal lattice, but these movements are elastic deformations and, as described in Chapter 5, elastic deformation is recoverable (i.e., nonpermanent). The movement of a glacier or the formation of a fold, however, is a permanent feature that represents ductile deformation. If we were to carefully remove a folded layer from an outcrop, or a deformed mineral from a hand specimen, they would not jump back to their original shapes. The distortions that occurred must be a result of permanent changes in the material. The principles that underlie the ability of materials like rocks to accumulate permanent strain are contained in a vast and ever-growing body of materials science literature. Structural geologists have increasingly applied concepts from materials science to geologic environments. The associated terminology, however, has not always remained consistent between these fields. In trying to keep new terms and concepts to a minimum, we've chosen to limit the coverage in this chapter; otherwise we'd lose sight of our ultimate goal: understanding the way rocks deform in the ductile regime.

In Chapter 5 we first introduced the concept of *flow.* At that point we described the topic merely in terms of stress and strain rate. We contrasted linear viscous (Newtonian) and nonlinear viscous (non-Newtonian) behavior, using analogs and simple mechanical models. In this chapter we turn to the physical processes

FIGURE 9.1 North-verging recumbent fold in mesozoic rocks of the Morcles thrust (or *Nappe*); Swiss Alps.

that allow materials to undergo appreciable, permanent distortions. To refresh your memory—strain that is distributed over the body rather than localized is what distinguishes *ductile behavior* from *brittle behavior*. But strain that appears homogeneous on one scale may represent heterogeneity on another, so again we need to include the scale of our observation. As scales of observation in structural geology range from nanometers (10^{-9} m) to kilometers, single minerals to mountain ranges, we define ductile behavior as uniform flow down to the scale of the hand specimen, that is, down to the mesoscopic scale.

We distinguish three fundamental mechanisms that produce ductile behavior in rocks and minerals: (1) **cataclastic flow,** (2) **diffusional mass transfer,** and (3) **crystal plasticity.** Which processes dominate at a given time in a rock's history is primarily a function of temperature, stress, strain rate, grain size, composition, and fluid content. Temperature, in particular, is an important parameter, but different minerals behave ductilely at different temperatures. What is considered high-temperature behavior for one mineral is low-temperature behavior for another mineral. Thus, when talking about the relationship between temperature and deformation, we introduce a normalized parameter that is called the **homologous temperature,** T_h. The homologous temperature is a dimensionless parameter that is defined as the absolute temperature divided by the absolute melting temperature of the material:

$$T_h = T/T_m \qquad \text{Eq. 9.1}$$

where T is temperature and T_m is melting temperature of the material, both in K (kelvins). We loosely define low-temperature conditions as $0 < T_h < 0.3$, medium-temperature conditions as $0.3 < T_h < 0.7$, and high-temperature conditions as $0.7 < T_h < 1$.

After discussing the fundamental mechanisms and their associated microstructures (i.e., mineral geometries on the microscopic scale), we close this chapter by examining the interrelationship between the various rheologic parameters (such as stress and strain rate; see Chapter 5), and by introducing the powerful concept of deformation mechanism maps. Let us first turn to the three mechanisms of ductile behavior—cataclastic flow, dislocation movement, and diffusion.

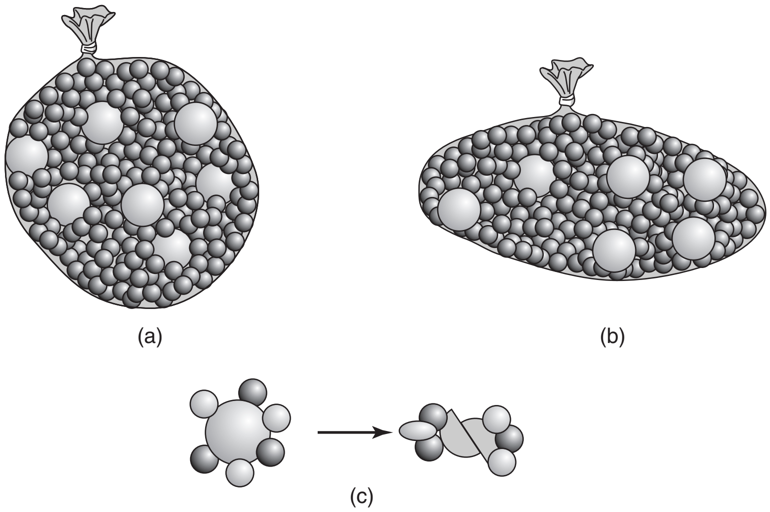

FIGURE 9.2 Bean bag experiment. Changing the shape of a bag is accomplished by the grains sliding past one another (a and b). Large grains may fracture and slide on the fracture surface (c).

9.2 CATACLASTIC FLOW

We start our examination of cataclastic flow with a simple experiment. Consider a bean bag that is originally shaped like a ball (Figure 9.2). We squash the bag so that it fits into a cube. In order for the ball-shaped bag to change shape, the beans have to slide past one another. Now imagine that the bag is strong and that you attach it to a winch that pulls the bean-filled bag through an opening that is smaller than a single bean. For the bag to pass through the small opening, all the individual beans must fracture into smaller pieces (brittle deformation), but the bag as a whole remains coherent. Such a process, where a mesoscopic body (the bean bag) changes shape without breaking into separate pieces, but the constituents (the beans) fracture into smaller pieces and/or slide past one another, is called **cataclastic flow.** In rocks, the tiny fractures are called microcracks and the pieces move past one another by the process of frictional sliding (see Chapter 6).

During cataclastic flow a rock deforms without obvious strain localization on the scale of the hand specimen, yet the *mechanism* of deformation is (micro)fracturing and/or frictional sliding (Figure 9.3). You may now better appreciate the confusion surrounding the terms brittle and ductile (Chapter 5). Cataclasis is mesoscopic ductile behavior, yet the process by which it occurs is microscopic brittle fracturing and frictional sliding!

In rocks, microfractures may occur at grain boundaries (intergranular) or within individual grains (intragranular). In both cases the process occurs by breaking many atomic bonds at the same time. The crystal structure away from the fracture, however, remains unaffected. Frictional sliding is strongly dependent on pressure; with increasing pressure the ability of sliding to occur is reduced (see Chapter 6). Therefore, we expect to find cataclastic flow in rocks only at relatively low lithostatic pressures. This condition is met in the upper several kilometers of the crust and, indeed,

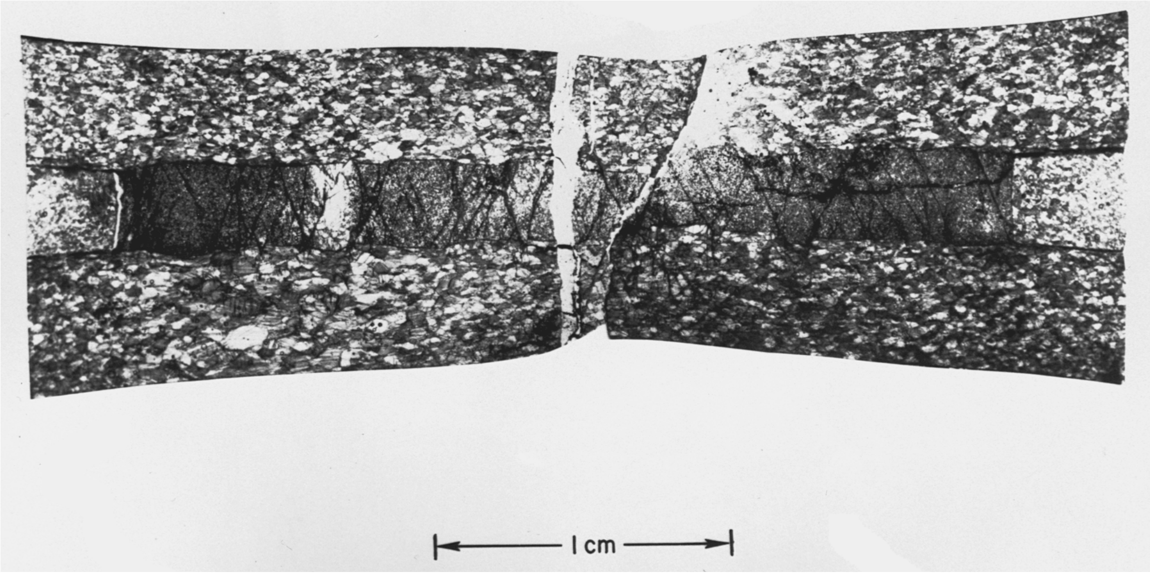

FIGURE 9.3 Extension experiment showing cataclastic flow in Luning dolomite (Italy) that is surrounded by marble that deformed by crystal plastic processes. This contrasting behavior reflects the relative strength of the materials.

we typically find cataclastic flow in shallow-crustal rocks, such as fault zones. The stress-dependence of cataclasis is one characteristic that distinguishes it from ductile mechanisms involving crystal defects, which are discussed in the next section.

9.3 CRYSTAL DEFECTS

Ductile behavior of materials at elevated temperatures is achieved by the motion of crystal defects. In simple terms, a crystal defect is an error in the crystal lattice, and there are three basic types: (1) **point defects,** (2) **line defects** or **dislocations,** and (3) **planar defects** or stacking faults. The motion of defects gives rise to permanent strain without the material losing cohesion (i.e., without fracturing). Point and line defects are most important for the deformation of rocks. Planar defects, which arise from errors in the internal layering of minerals, play only a limited role in deformation. In order to understand diffusional mass transfer and crystal plasticity, we first need to take a more detailed look at point and line defects.

9.3.1 Point Defects

There are two types of point defects: (1) **vacancies** and (2) **impurities.** Vacancies are unoccupied sites in the crystal lattice (Figure 9.4a). Impurity atoms are (a) **substitutionals,** in which an atom in a lattice site of the crystal is replaced by a different atom (Figure 9.4b), and (b) **interstitials,** in which an atom is at a nonlattice site of the crystal (Figure 9.4c). Vacancies can migrate by exchange with atoms in neighboring sites (Figures 9.4d). At first glance, the concept of migrating vacancies sounds a bit odd, but when an atom moves into a vacant site, you can equally say that the vacancy moved. The general term for this process of atom or vacancy migration is diffusion. This important process is discussed later in the chapter. When we apply a differential stress to a crystal, this causes a gradient in the vacancy concentration. Vacancies migrate down these concentration gradients, which causes material to deform ductilely, or to flow.

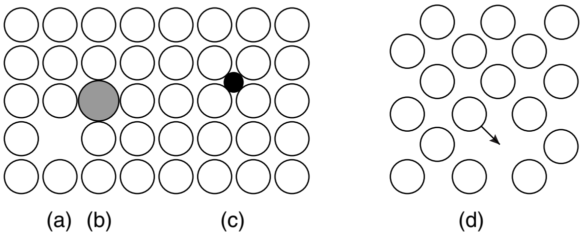

FIGURE 9.4 Point defects: (a) vacancy, (b) substitutional impurity, (c) interstitial impurity, (d) vacancy migration.

9.3.2 Line Defects or Dislocations

A line defect, usually called a **dislocation,** is a linear array of lattice imperfections (Figure 9.5). More formally, a dislocation is the linear array of atoms that bounds an area in the crystal that has slipped relative to the rest of the crystal (Figure 9.6). This definition is hardly informative at this point, so we first look at the geometry of two end-member configurations, the edge dislocation and the screw dislocation, before turning to the concept of slip in crystals.

An **edge dislocation** occurs where there is an extra half-plane of atoms in the crystal lattice. As illustrated in Figure 9.7a, there are 7 vertical planes of atoms at the top half of the crystal and only 6 vertical planes of atoms at the bottom half. The termination of the *extra half-plane* (the plane that ends halfway in the crystal) is the dislocation. It extends into the crystal as the

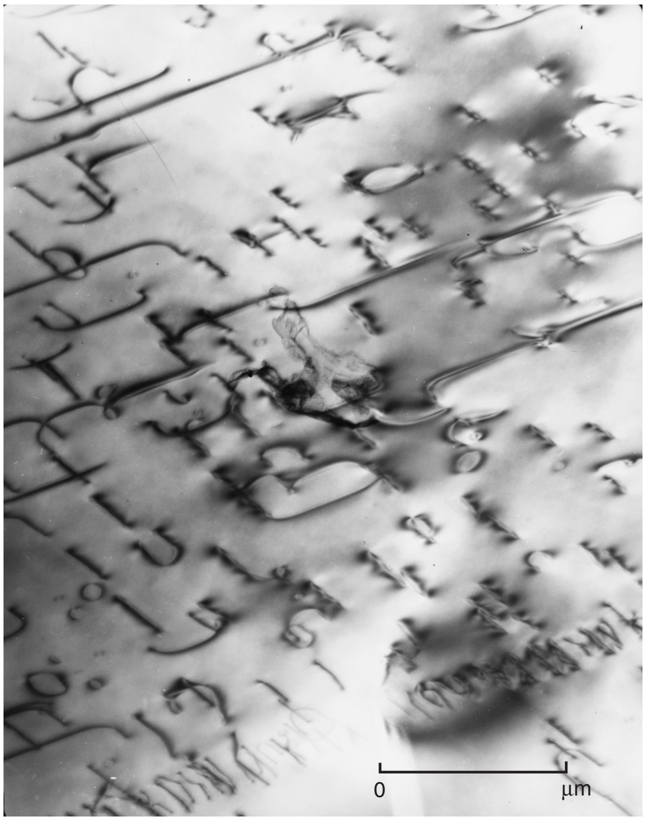

FIGURE 9.5 Transmission electron micrograph showing dislocation lines, loops, and arrays in experimentally deformed olivine.

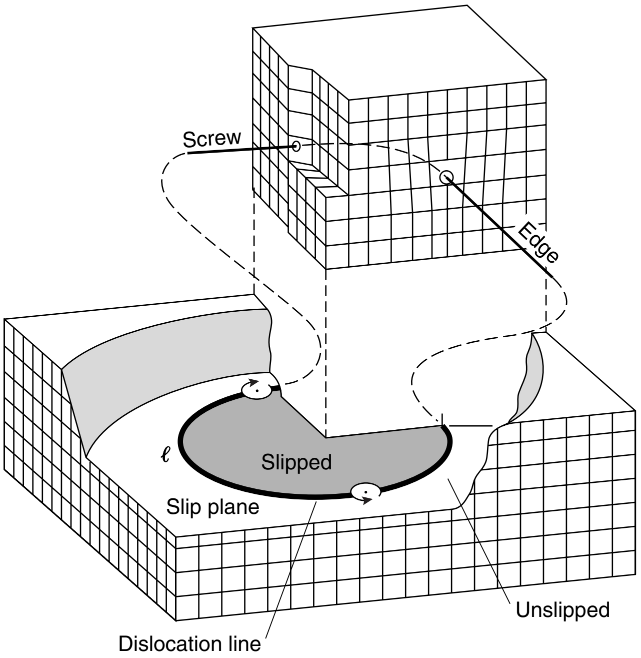

FIGURE 9.6 Geometry of a dislocation showing the edge- and screw-type dislocations and their geometrical relationship. The boundary between the unslipped and slipped portion of the crystal is the dislocation line, **l.**

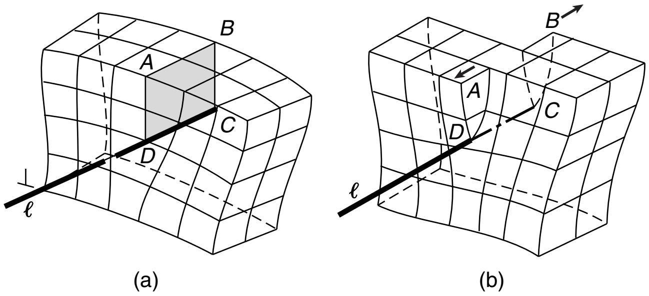

(a) (b)

FIGURE 9.7 Types of dislocations. (a) The extra half-plane of atoms in an edge dislocation. (b) The corkscrew-like displacement of the screw dislocation. The dislocation line, **l,** is marked.

dislocation line, **l** (line *CD* in Figure 9.7a). The symbol for an edge dislocation is ⊥ or ⊤, depending on whether the location of the extra half-plane is above or below the associated glide plane of the crystal (see further). Imagine an axe that is stuck in a piece of wood. The presence of a dislocation causes a distortion of the crystal structure, just like a wedge distorts the log that is being split.

In **screw dislocations,** the atoms are arranged in a corkscrew-like fashion (Figure 9.7b); the axis of the screw marks the dislocation line (line *CD* in Figure 9.7b). A useful analogy of the geometry of a screw dislocation is a car parking deck, in which ramps carry cars up or down to individual floors. Many geologists, however, prefer a corkscrew analogy.

In a deformed crystal, an atom-by-atom circuit around the dislocation fails to close by one or more atomic distances, while a similar circuit around atoms in a perfect crystal would be complete. The arrow connecting the two ends of the incomplete circuit is called the **Burgers vector, b.** The length of the Burgers vector in most minerals is on the order of nanometers ($1 \text{ nm} = 1 \times 10^{-9}$ m). For an edge dislocation, the Burgers circuit remains in the same plane (Figure 9.8a), while for a screw dislocation the circuit steps up or down to another plane (Figure 9.8b). Edge and screw dislocations can, therefore, be distinguished on the basis of the relationship between the Burgers vector

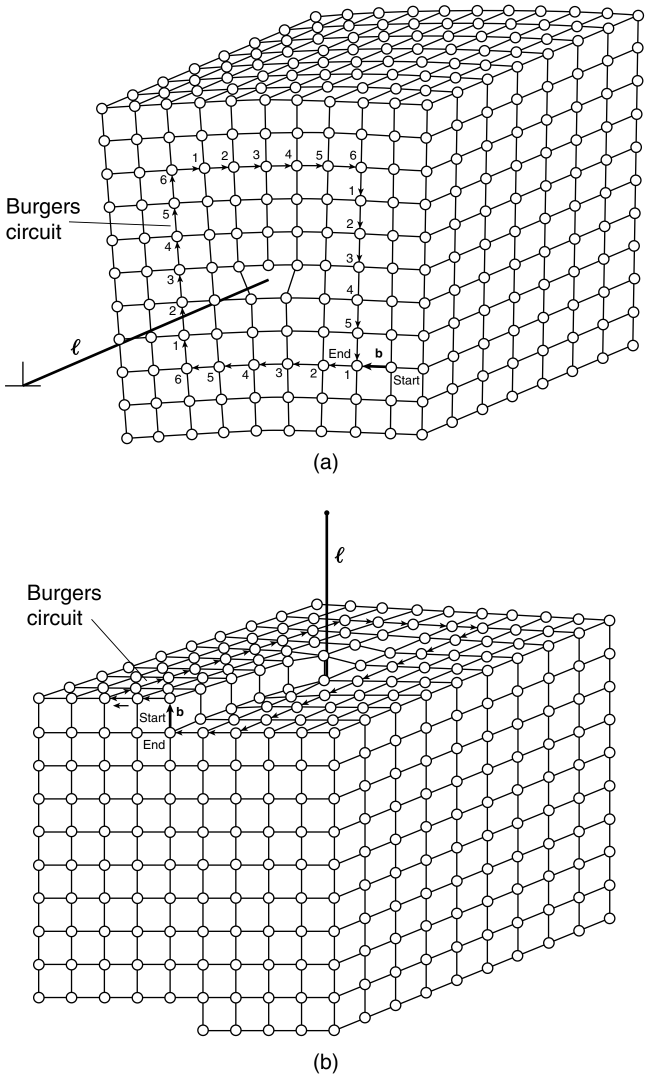

(a)

(b)

FIGURE 9.8 Determination of the Burgers vector, **b,** of a dislocation using a Burgers circuit. (a) The Burgers circuit around an edge dislocation (marked by **l**). (b) The Burgers circuit in a screw dislocation. The closure mismatch for both edge and screw dislocations is the Burgers vector, **b.** In the edge dislocation **b**⊥**l,** and in the screw dislocation **b**//**l.**

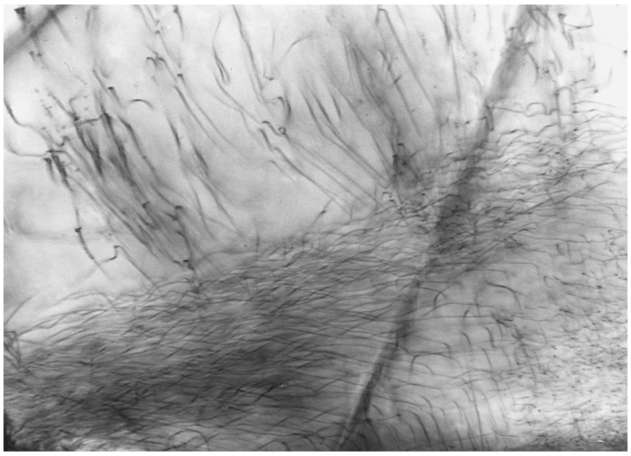

FIGURE 9.9 Dislocations in olivine from a Hawaiian mantle nodule. The dislocations appear by a decoration technique (described in the appendix), which allows for optical inspection. Width of view is ~200 μm.

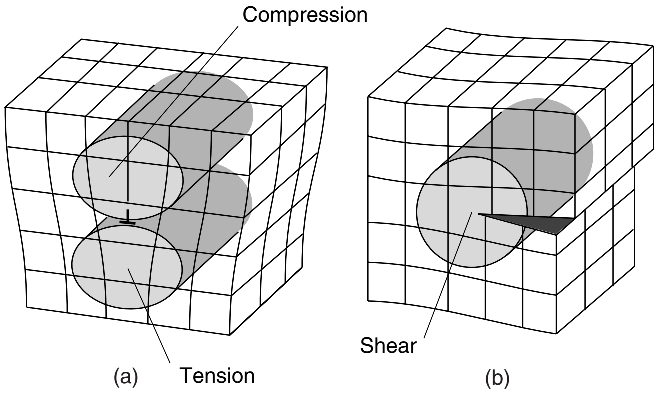

FIGURE 9.10 Geometry of the stress field (shaded region) around an edge dislocation (a) and around a screw dislocation (b).

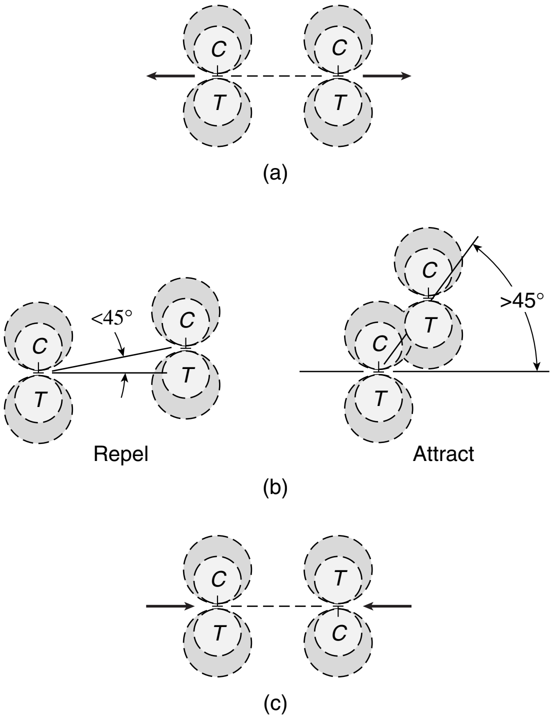

FIGURE 9.11 Interactions between neighboring edge dislocations. Regions labeled *C* and *T* are areas of compression and tension, respectively, associated with each dislocation. (a) Like dislocations on the same or nearby glide planes repel. (b) Like dislocations on widely separated glide planes may attract or repel depending on the angle between the lines joining the dislocations. (c) Unlike dislocations on the same or nearby glide planes attract.

and the dislocation line. For edge dislocations, the Burgers vector is *perpendicular* to the dislocation line, (Figure 9.8a) and for screw dislocations, the Burgers vector is *parallel* to the dislocation line (Figure 9.8b). These properties are used to determine the nature of imaged dislocations revealed by the electron microscope (see Section 9.8). Edge and screw dislocations are only end-member geometries; dislocations that consist of part edge and part screw components are called **mixed dislocations.** Besides being visible at very large magnifications in the electron microscope, crystal defect features may be indirectly seen by using a decoration technique (see appendix at the end of this chapter). Figure 9.9 shows an optical image of dislocations in the mineral olivine using a decorated sample.

Earlier we mentioned that the presence of dislocations distorts the crystal lattice, which gives rise to a local stress field around a dislocation. In an edge dislocation (Figure 9.10a) there is compressive stress on the side of the extra half-plane of atoms and tension on the opposite side. The earlier wood-splitting analogy serves to illustrate this pattern. The axe forces the wood apart, giving rise to compression, which may result in the axe becoming stuck. Just beyond the tip of the blade, however, there is tension, which is why you can split wood without the blade going all the way through. Similarly, in a screw dislocation we introduce shear stresses (Figure 9.10b). What is the effect of these local stresses? The role of compressive and tensile stresses is analogous to the behavior of magnets and charged particles. The compressive stress fields of edge dislocations repel, while the compressive and tensile fields of edge dislocations attract (Figure 9.11), just like the poles of two magnets attract or repel when their polarities are reversed. Similarly, screw dislocations with the same sense of shear repel each other and those with opposite senses of shear attract. In a crude way you can say that dislocations are able to “see” each other by the stress fields they generate from the distortion of the crystal lattice. Later we will see that these stress fields permit dislocations to move, producing permanent distortions of the crystal, while lowering the internal strain energy. Remember that this internal strain energy is not the same as the applied stress arising from, for example, squeezing a crystal.

Edge and screw dislocations are end-member configurations, called **perfect dislocations,** because the Burgers vector has a length of one unit lattice distance (i.e., the length of one atomic bond, or multiples thereof). However, studies of minerals (e.g., calcite) have shown Burgers vectors that differ from one unit lattice distance; these are called *partial dislocations.* Partial dislocations may be formed by splitting a long Burgers vector into two or more components by the process of **dissociation.** Dissociation is energetically more favorable because it allows smaller displacements. Arrays of partial dislocations produce, for example, twinning in crystals (see Section 9.4).

9.4 CRYSTAL PLASTICITY

Dislocations are able to migrate through the crystal lattice if the activation energy for movement is achieved. The distortion of the crystal lattice around dislocations is one source of driving energy, as the system tries to achieve a lower internal strain energy. Applying a differential stress is another driving mechanism for dislocation motion. The associated distortion of solid phases is called crystal plasticity. Dislocation movement may occur by **glide** and a combination of glide and climb (**creep**), depending mainly on temperature. A third case of crystal-plastic behavior, **twinning,** occurs at low temperatures in some minerals.

9.4.1 Dislocation Glide

Deformation and temperature introduce energy into the crystal, which allows dislocations to move. However, dislocations are not free to move in any direction through the crystal. At low temperatures they are restricted to **glide planes** (or **slip planes**). The glide plane of a dislocation is the plane that contains the Burgers vector, **b,** and the dislocation line, **l.** Because a plane is defined by two nonparallel lines, each edge dislocation has one slip plane, because **b** and **l** are perpendicular. A screw dislocation on the other hand has many potential slip planes, because **b** and **l** are parallel. In crystallographic terms, a glide plane is a crystallographic plane across which bonds are relatively weak. Some crystals have only one crystallographic plane that is an easy glide plane; others may have many. Table 9.1 lists the dominant slip systems for some of the more common rock-forming minerals. Note that in many crystals more than one slip system may be active under similar conditions.

What is the actual process that allows the movement of dislocations? Nature has devised an energetically clever way for dislocations to move. Rather than simultaneously breaking all atomic bonds across a plane, such as occurs during fracturing, only bonds along the dislocation line are broken during an increment of movement. This requires much less energy than fracturing. Let us again turn to an analogy to illustrate this. The movement of dislocations is comparable to moving a large carpet across a room that contains heavy pieces of furniture. The easiest way to move the rug is to ruck up one end and propagate the ruck across the room. Energy is only needed to lift up selected furniture legs to propagate the ruck past these obstacles rather than lift all the furniture simultaneously. In nature, caterpillars and snakes move similarly by displacing one segment of their body at a time, instead of moving their entire body simultaneously. Edge dislocations move by successive breaking of bonds under the influence of a minimum stress acting on the glide plane, which is called the **critical resolved shear stress** (CRSS). If a crystal has several potential glide planes, it is likely that, for a given applied stress, the CRSS is exceeded on at least one and sometimes more than one of these glide planes. An edge dislocation moves when the unattached atoms at the bottom of the extra half-plane bond to the next atoms that are located directly below the glide plane. Thus the position of the extra half-plane moves relative to the dislocation without breaking all bonds in the extra half-plane (Figure 9.12a). A screw dislocation moves forward by shearing one atomic distance (Figure 9.12b), similar to tearing a piece of paper. While atomic bonds are broken and reattached when dislocations move toward the edge of a crystal, they leave a perfect crystal lattice behind. When a dislocation reaches the edge of the grain there are no more atoms below to attach to and the crystal becomes offset. This offset of the crystal edge produces stair-step structures on the surface of the crystal known as **slip bands,** which are sometimes visible on large crystal surfaces. Thus, the process of dislocation movement produces permanent strain without the material ever losing coherency.

9.4.2 Cross-Slip and Climb

It is not always possible for dislocations to propagate to the edge of the crystal. Point defects, such as impurity atoms that are bonded tightly to their neighbors, can resist the breaking of bonds that is required for dis-

TABLE 9.1 **DOMINANT SLIP SYSTEMS IN COMMON ROCK-FORMING MINERALS**

Mineral	Glide plane and slip direction[a]	Comments
Calcite	$\{\bar{1}018\}\langle 40\bar{4}1\rangle$	e-twinning
	$\{10\bar{1}4\}\langle\bar{2}021\rangle$	r-twinning
	$\{10\bar{1}4\}\langle\bar{2}021\rangle$	r-glide
	$\{01\bar{1}2\}\langle 2\bar{2}01\rangle$ or $\langle\bar{2}021\rangle$	f-glide
Dolomite	$\{\bar{1}012\}\langle 10\bar{1}1\rangle$	f-twinning
	$(0001)\langle 2\bar{1}\bar{1}0\rangle$	c-glide
	$\{01\bar{1}2\}\langle 2\bar{2}01\rangle$ or $\langle\bar{2}021\rangle$	f-glide
Mica	$(001)\langle 110\rangle$	basal (c) slip
Olivine	$(001)[100]$	
	$\{110\}[001]$	
Quartz	$(0001)\langle 11\bar{2}0\rangle$	basal (c) slip
	$\{10\bar{1}0\}[0001]$	prism (m) slip, along c
	$\{10\bar{1}0\}\langle 11\bar{2}0\rangle$	prism (m) slip, along a
	$\{10\bar{1}1\}\langle 11\bar{2}0\rangle$	rhomb (z) slip

[a] Miller indices for equivalent glide planes from crystal symmetry are indicated by { }; specific glide planes are indicated by ( ); equivalent slip directions from crystal symmetry are indicated by < >; individual slip directions are indicated by [ ].

From: Wenk, 1985

location glide. Unfavorable stress fields of the dislocations themselves can also resist their motion, especially when many dislocations are present. Just consider trying to work your way past a car accident slowing the traffic in your lane, or even bringing it to a complete halt. Not surprisingly, obstacles that result from the presence of many immobile dislocations are called **pile-ups.** In order to overcome these obstacles, edge and screw dislocations must move out of their current glide plane, which they do by the processes of climb and cross-slip, respectively. The processes require additional energy beyond that for dislocation glide. Screw dislocations, unlike edge dislocations, are not confined to a single glide plane, because the dislocation line and Burgers vector are parallel. They can therefore leave one glide plane and move to another glide plane with relative ease, a process called **cross-slip** (Figure 9.13a). If it is so easy, why does cross-slip not occur all the time? Cross-slip requires that the dislocation abandons a favored glide plane (one with a short Burgers vector) for a less-favored one, and thus cross-slip takes place only if the CRSS on the less-favored plane is increased. Alternatively, raising the temperature lowers the CRSS that is needed for cross-slip, because atomic bonds are weakened, and cross-slip occurs more easily.

Edge dislocations cannot cross-slip because they have only one glide plane. However, they can **climb** to a different, parallel glide plane if there are vacancies to accept the lowest atoms of the extra half-plane (this is shown two-dimensionally in Figure 9.13b). Climb, therefore, involves diffusion (see further), and because the rate of vacancy production increases with rising temperature, the efficiency of dislocation climb is temperature dependent. Both cross-slip and climb are activated at temperature conditions that exceed those for dislocation glide in a mineral given the same stress conditions, and therefore they typically occur at deeper (i.e., hotter!) levels in the Earth. Although it is not possible to identify a fixed depth at which cross-slip and climb occur, because this is a function of the mineral as well as Earth's thermal structure, as a general guide, we can specify the temperature values at which these processes occur for different minerals. Glide and climb occur at temperatures greater than 300°C for quartzitic rocks and carbonates, and at

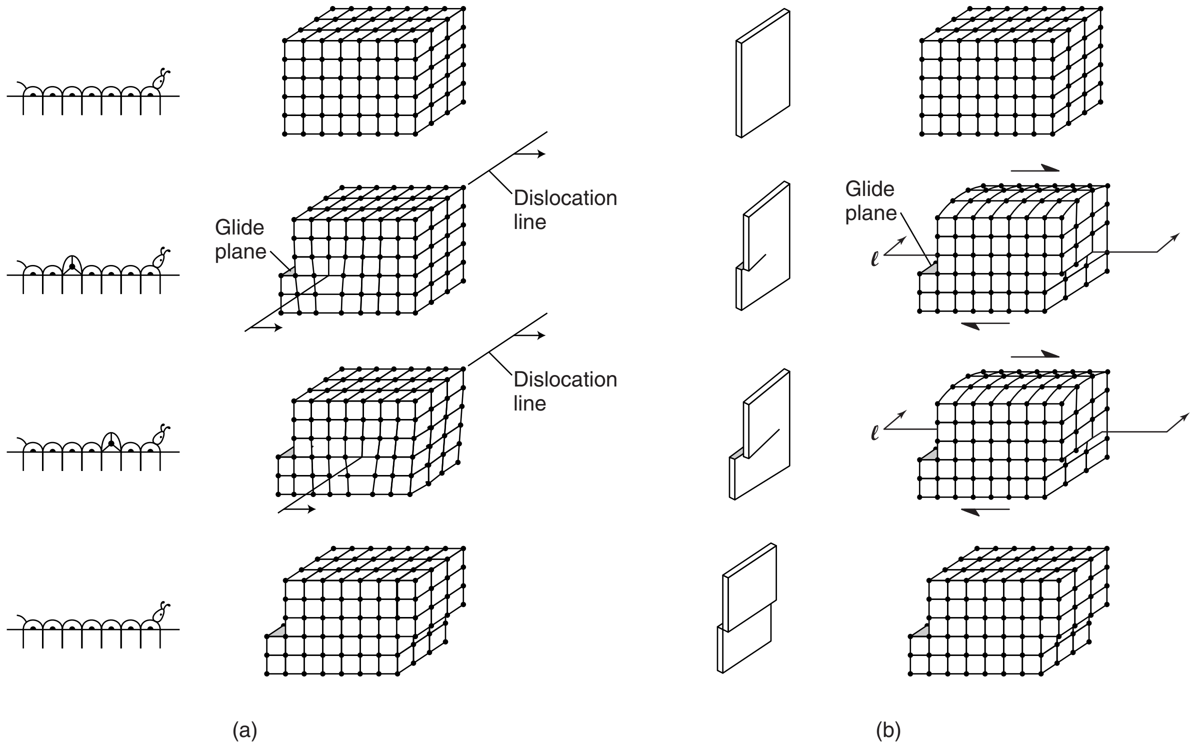

FIGURE 9.12 Dislocation glide. (a) Movement of an edge dislocation, which may be likened to the movement of a caterpillar. (b) Movement of a screw dislocation, which is analogous to tearing a sheet of paper, with the screw dislocation at the tip of the tear. After the dislocation passes through the lattice, it leaves behind a strained crystal with a perfect crystal lattice structure. The dislocation line, **l,** and the glide planes (shaded) are shown.

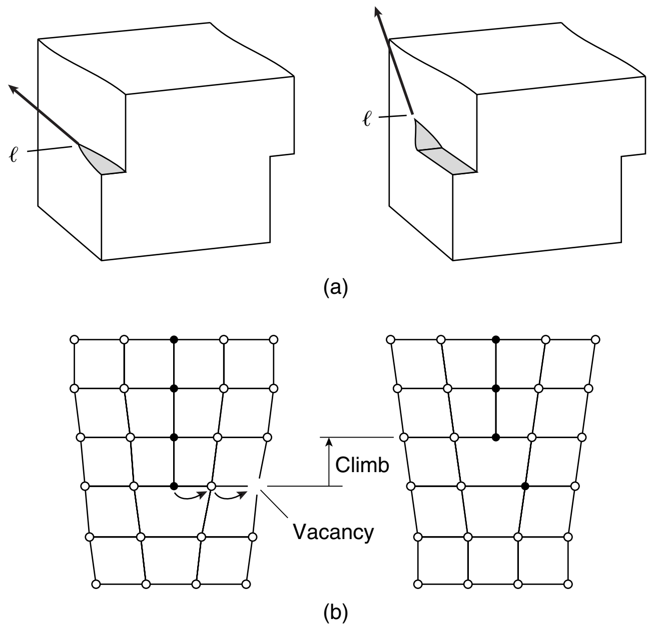

FIGURE 9.13 Cross-slip of a screw dislocation (a), and climb of an edge dislocation (b) by diffusion of atoms (arrows).

higher temperatures (>500°C) for such common minerals as dolomite, feldspar, and olivine. In the literature you find that the term **dislocation creep** is used for the combined activity of glide and climb.

While like dislocations often repel one another, unlike dislocations attract and may annihilate each other. **Dislocation annihilation** is one way of reducing the internal strain energy that arises from lattice distortions in a crystal. For example, two edge dislocations lying in the same glide plane with the extra half-plane of one dislocation inserted upwards (positive edge dislocation) and the other downward (negative edge dislocation) annihilate each other (Figure 9.14a). Similarly, convergence of screw dislocations with Burgers vectors in opposite directions also results in annihilation. Two dislocations of opposite sign but on different glide planes may still attract, but they cannot fully annihilate each other. In such cases, a point defect remains (such as a vacancy; Figure 9.14b). Because climb and cross-slip increase the probability of dislocation annihilation, the rate of dislocation annihilation is also temperature dependent.

9.4.3 Mechanical Twinning

Twins are a common feature in many minerals. You may see them with the hand lens in the minerals plagioclase and calcite. In thin section, under crossed polarizers, they are easily recognized by their extinction behavior and lathlike shape as you rotate the stage. Twins that develop during the growth of a crystal, called **growth twins,** say little or nothing about the conditions of deformation (i.e., stress and strain). In contrast, minerals such as calcite form twins in response to an applied stress; these are called **mechanical twins** (Figure 9.15). We'll first have a look at twinning in general and then see what information mechanical twins can provide for deformation studies.

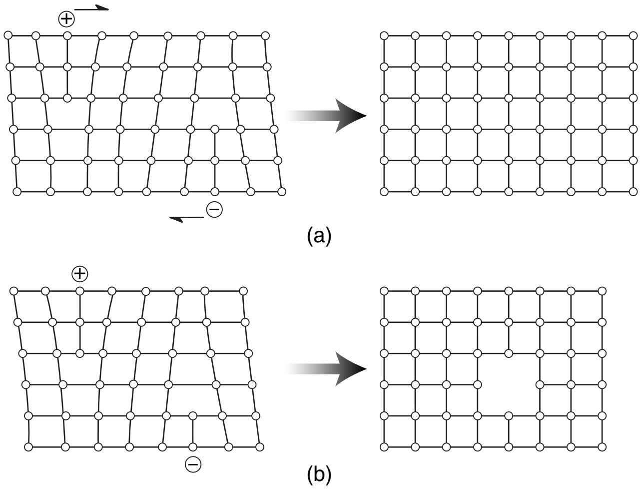

FIGURE 9.14 (a) Two edge dislocations with opposing extra half-planes that share a glide plane move in opposite direction to meet and form a perfect crystal. (b) When they move in different glide planes, a vacancy may be formed when they meet.

Mechanical twinning is a type of crystal plastic process that involves the glide of **partial dislocations.** A surface imperfection, the **twin boundary,** separates two regions of a twinned crystal. The lattices in these two portions are mirror images of each other; in other words, a twin boundary is a mirror plane with a specific crystallographic orientation. As a rule, twinning planes cannot already be mirror planes in the untwinned crystal, and mechanical twinning is therefore most common in low-symmetry minerals such as trigonal calcite and dolomite, and triclinic feldspar. Recall that crystal symmetry is a geometric operation that repeats a crystal plane in another position. For reference, Table 9.2 lists the seven crystal systems and their symmetries that you may have learned in your mineralogy and/or petrology class.

Mechanical twins are produced when the resolved shear stress acting on the future twin boundary exceeds a critical value (the CRSS for twinning). During twinning, the crystal lattice rotates in the direction that produces the shortest movement (smallest linear displacement) of atoms, with a unique rotation angle. As such, mechanical twinning has similarities with dislocation glide, but differs in two aspects. First, atoms are not moved an integral atomic distance as in glide, but

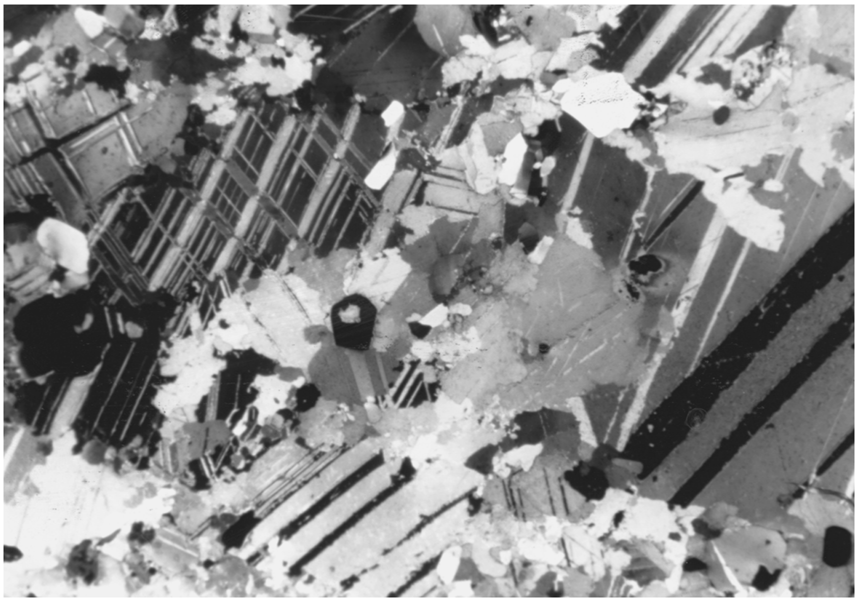

FIGURE 9.15 Calcite e-twins in marble from southern Ontario (Canada). Width of view is ~4 mm.

TABLE 9.2 **CRYSTAL SYSTEMS**

System	Symmetry	Crystal Axes
Triclinic	1 one-fold axis or center of symmetry	$a \neq b \neq c$, $\alpha \neq \beta \neq \gamma \neq 90°$
Monoclinic	1 two-fold axis or 1 symmetry plane	$a \neq b \neq c$, $\alpha = \gamma = 90°$, $\beta \neq 90°$
Orthorhombic	3 two-fold axes or 3 symmetry planes	$a \neq b \neq c$, $\alpha = \beta = \gamma = 90°$
Trigonal	1 three-fold axis	$a_1 = a_2 = a_3 \neq c$, $\beta = 90°$
Hexagonal	1 six-fold axis	$a_1 = a_2 = a_3 \neq c$, $\beta = 90°$
Tetragonal	1 four-fold axis	$a = b \neq c$, $\alpha = \beta = \gamma = 90°$
Cubic	4 three-fold axes	$a = b = c$, $\alpha = \beta = \gamma = 90°$

a, b, c describes the length of the crystal axes; α is the angle between *b* and *c;* β is the angle between *a* and *c;* γ is the angle between *a* and *b.*

rather only by some fraction of the atomic distance; consequently, twinning involves partial dislocations. Secondly, the twinned portion of a grain is a mirror image of the original lattice (Figure 9.16a), whereas the slipped portion of a grain has the same crystallographic orientation as the unslipped portion of the grain (Figure 9.16b). For deformation studies we are interested mostly in mechanical twinning; that is, twins produced by stress. We digress briefly to explore one application using the mineral calcite.

The fact that twinning takes place along specific crystallographic planes in a calcite crystal,[1] and that rotation occurs over a specific angle and in a specific sense, allows us to use twinning as a measure of finite strain and differential stress. The atomic structure of calcite twins is illustrated in Figure 9.17. (Note the specified rotation angle of the crystallographic *c*-axis, which is perpendicular to the planes containing the CO_3 groups, and that of the crystal face.) In Figure 9.18a, a deformed grain *A′B′CD* with one twin is shown; the original grain outline is *ABCD,* whose sides are parallel to calcite crystal planes. From this figure you can see that the shear strain for the twinned grain is

$$\gamma = \tan \psi = q/T \qquad \text{Eq. 9.2}$$

For one twin, $q = p$, so

$$\gamma = \frac{2t \tan(\phi/2)}{T} \qquad \text{Eq. 9.3}$$

---

[1] We will only consider e-twins ({1018}<4041>) with a rotation angle for the *c*-axis of 52.5°, and a CRSS of 10 MPa.

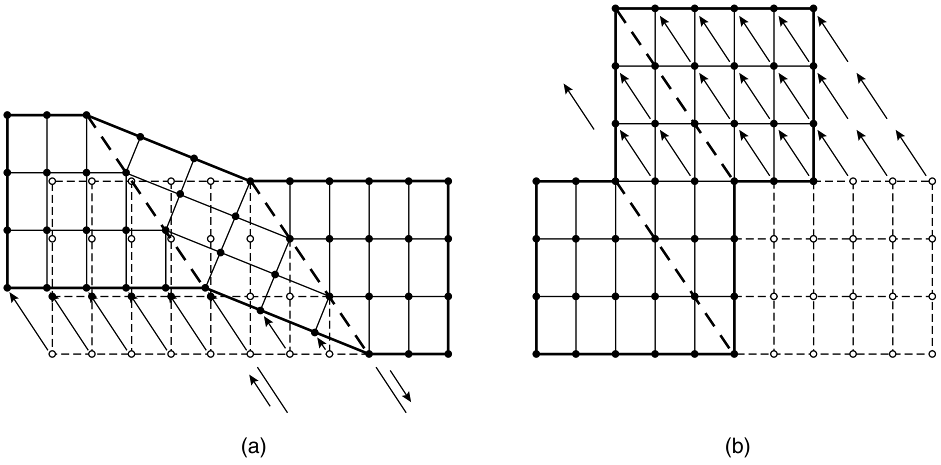

FIGURE 9.16 Schematic illustration of mechanical twinning (a). The heavy outline marks a twinned grain, in which the twin boundaries (heavy dashes) are mirror planes. The atomic displacements are of unequal length and generally do not coincide with one atomic distance. Closed circles are atoms in final structure and open circles give the original positions of displaced atoms. Twinning contrasts with dislocation glide (b), in which atoms move one or more atomic distances in the glide plane (heavy dashed line).

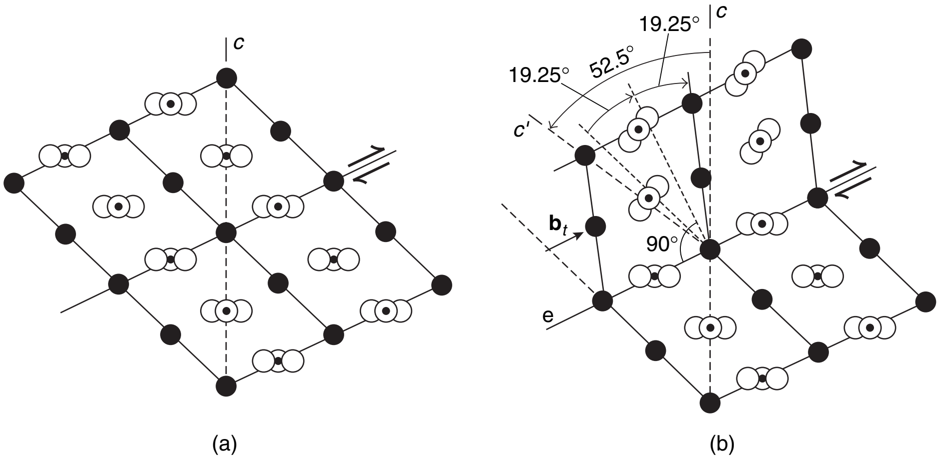

FIGURE 9.17 Calcite crystal lattice showing layers of Ca (large black dot) and CO_3 groups (C is small dot, O is large open circle); the crystallographic *c*-axis is marked (a). The twinned calcite lattice in (b) shows the partial dislocation ($\mathbf{b}_t$) and angular rotations of the *c*-axis and the crystal face.

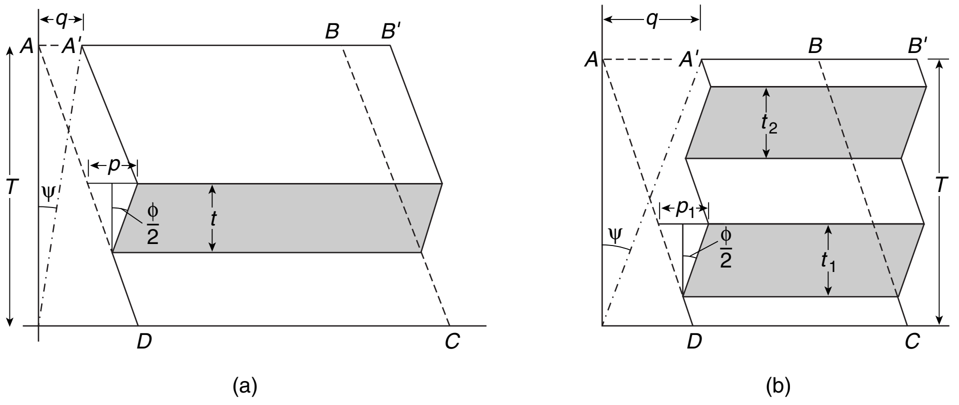

FIGURE 9.18 Calcite strain-gauge technique. An original grain *ABCD* (a) with a single twin of thickness, *t* (shaded region). In (b) a grain with multiple twins (shaded regions) is shown.

where T is the grain thickness and t is the twin thickness. For a grain containing several twins (Figure 9.18b) the shear strain is obtained by adding the strain due to each twin, or

$$\gamma = \frac{2}{T}\sum_{i=1}^{n} t_i \tan\ (\phi/2) \qquad \text{Eq. 9.4}$$

where n is the number of twins in the grain. Given that the angle ϕ is constant in the case of calcite (≈38°; Figure 9.18b), Equation 9.4 simplifies to

$$\gamma = \frac{0.7}{T}\pi\sum_{i=1}^{n} t_i \qquad \text{Eq. 9.5}$$

So, if we measure the total width of twins and the grain size perpendicular to the twin plane we can obtain the total shear strain for a single twinned grain. In an aggregate of grains, the shear strains will vary as a function of the crystallographic orientation of individual grains relative to the bulk strain ellipsoid, and we use this variation to determine the orientation of the principal strain axes by determining the orientations for which the shear strains are zero[2] and maximum. This strain analysis technique is called the **calcite strain-gauge method.** Looking again at Figure 9.18 and Equation 9.5, we can now determine the maximum amount of shear strain that can be accumulated using twinning: γ_{max} occurs when the entire grain is twinned, so $t = T$; thus, $\gamma_{max} = 0.7$, or $X/Z \approx 2$. This maximum contrasts with the amount of strain that can accumulate during dislocation glide, which is unrestricted. Moreover, methods for the determination of the differential stress for an aggregate with twinned grains have been developed that use the number of activated twin planes. Thus, calcite twinning analysis can give both strain and differential stress magnitudes for naturally deformed carbonates.

The calcite strain-gauge technique has proven to be very useful in studying stress and strain fields in limestones that were subjected to small strains, the kinematics of folding, the formation of veins, the early

---

[2] Details of the method are described elsewhere, and a computer routine is normally used for the analysis.

deformation history of fold-and-thrust belts, and even deformation patterns in continental interiors. The great advantage of this method lies in the fact that twinning occurs at low homologous temperature and low differential stress, and that the orientation and magnitude of even small finite strains are recorded.

9.4.4 Strain-Producing versus Rate-Controlling Mechanisms

We saw previously that dislocations are not stationary elements of a crystal, but are able to move (glide), and that they leave behind what is called the *slipped portion* of the crystal. Perhaps surprisingly, this slipped portion has no crystallographic distortion after the dislocation has passed through this part of the crystal. This ability of dislocation to move through a crystal brings us back to the earlier definition of a dislocation that was given without much explanation at the time (Section 9.3): a dislocation is the linear array of atoms that bounds an area in the crystal that has slipped one Burgers vector more than the rest of the crystal. Having examined the various dislocation motion mechanisms, we need to recognize an important distinction between dislocation glide on the one hand, and dislocation cross-slip and climb on the other hand. Dislocation glide is the process that produces a change in the shape of grains; it is therefore the main **strain-producing mechanism** of crystal plasticity. Cross-slip and climb facilitate dislocation glide, but by themselves produce little finite strain; they allow a dislocation to leave its original glide plane, to bypass an impurity, for example. Cross-slip and climb are therefore the **rate-controlling mechanisms** of crystal plasticity, and limit the resulting strain rate. Because climb occurs at temperatures that are higher than those required for glide in a mineral, you also find the terms **low-temperature creep** for dislocation glide (and twinning) and **high-temperature creep** for dislocation glide plus climb.

9.4.5 Where Do Dislocations Come From?

Nothing in life is perfect! You have undoubtedly heard and probably experienced this yourself, and the same goes for a mineral's life. Defects, such as dislocations, are a part of all minerals, for good reasons: The small offsets that occur at the edges of crystals containing dislocations (on the order of nanometers) are used as nucleation sites during mineral growth; while for deformation, dislocations are necessary to enable the shape change during crystal plasticity. So far, we have only talked about the situation where a couple of dislocations occur at the same time, but the number of dislocations in a mineral, the **dislocation density,** *N,* is actually quite large. For example, "perfect" grains that have grown from a melt have a dislocation density of 10^6 cm^{-2}, and this density is several orders of magnitude larger in deformed grains. Even near perfect crystals that are grown in the laboratory still have hundreds of dislocations per square centimeter (cm^2). So what is this strange unit "cm^{-2}" for dislocation density? Dislocation density, *N,* describes the total length of dislocations per volume of crystal; thus N = length/volume, so the unit of N is $[l]/[l^3] = [l^{-2}]$. Measuring dislocation length per unit volume is not a very convenient way to determine *N,* so practically we measure the number of dislocations (dimensionless scalar) that intersect an area (l^2), which gives the unit [l^{-2}]. Later, in Section 9.9, we will give an example of a dislocation density calculation.

In order to obtain appreciable strains from dislocation movement, we will need a great many dislocations. We have already learned that strain is produced by dislocations moving to the edge of the crystal (Figure 9.12), leaving a perfect lattice behind. So, in order for crystal plastic processes to proceed we actually need to generate dislocations. We earlier mentioned that dislocation density is greater in strained grains than in unstrained, "perfect" grains, which suggests that dislocations are generated during deformation. One mechanism for dislocation generation (or multiplication) is by **Frank-Read sources** (Figure 9.19). Consider a dislocation that is anchored at two points, *A* and *B;* this pinning may arise from impurities, climb, or interaction with other dislocations (not shown in the figure). During glide, the *A–B* dislocation will bow out because it is pinned at its edges (Figure 9.19b–d), and eventually this produces the kidney-shaped loop in Figure 9.19e and 9.19f. Note that the dislocation segments at *a* and *b* in Figure 9.19f are opposite in sign because their Burgers vectors are opposite. So as *a* and *b* come together they annihilate (Figure 9.19g), forming a new *A–B* dislocation line, while leaving the old loop present (Figure 9.19h). The process starts again for the new *A–B* dislocation line while the first loop continues to glide. Because there is no restriction on the number of cycles, a great many dislocation loops are generated in this manner, which occurs for both edge and screw dislocations. This and other dislocation multiplication mechanisms collectively produce the high dislocation densities that are required for grains to deform by crystal plastic processes.

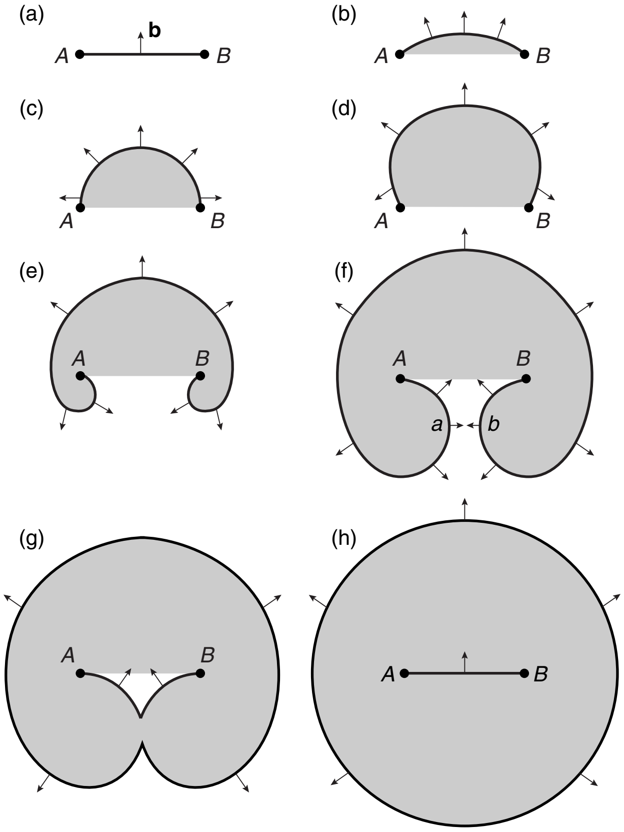

FIGURE 9.19 Dislocation multiplication in a Frank-Read source. (a) A pinned dislocation with Burgers vector, **b**, bows out during glide (b–g) to form a new dislocation (h). The slipped portion of the grain is shaded.

9.5 DIFFUSIONAL MASS TRANSFER

Flow of rocks also occurs by the transfer of material through a process called **diffusion.** We'll discuss three diffusion-related deformation mechanisms that are important for natural rocks: (1) **pressure solution,** (2) **grain-boundary diffusion,** and (3) **volume diffusion.** Diffusion occurs when an atom (or a point defect) migrates through a crystal. The process is strongly temperature dependent, because thermal energy causes atoms to vibrate, facilitating the breaking and reattachment of bonds. Increasing the temperature of a material proportionally increases the ability of individual atoms to jump to neighboring vacant sites. For example, at the melting temperature of Fe ($T_h = 1$), the **jump frequency,** Γ, of vacancies is on the order of 10^{10} per second. The jump distance, r (the distance between atoms in the crystal structure), for each jump is 10^{-10} m (0.1 nm). We can determine the average area, R^2, for a vacancy by Einstein's equation:[3]

$$R^2 = \Gamma t r^2 \qquad \text{Eq. 9.6}$$

where t = time. If we use $t = 1$ s, then $R^2 = 0.1$ mm^2, at $T_h = 1$ for Fe metal. This area seems small, so you might think at first that the process is relatively insignificant. However, considering that geologic time is measured in millions of years, the value of R^2 becomes quite large. For example, at $t = 1$ m.y. (3.1×10^{13} s) the value of R^2 is >3000 m^2. Such areas, however, are only representative for minerals in rocks near their melting temperature, which is not the typical condition during rock deformation. At lower T_h, diffusion distances are orders of magnitude less. Another aspect of diffusion that needs to be appreciated is that R^2 does not define the linear distance between the original position of an atom and its position after time t. Diffusion is nondirectional in an isotropic stress field; it is, what we call, a **random-walk process.** So the final distance traveled is distinct from the path and area covered.

Theoretical arguments, which we will not discuss here, define a diffusion coefficient, D, for a given mineral, describing movement of a species down a concentration gradient:[4]

$$D = (\Gamma/6)\, r^2 \qquad \text{Eq. 9.7}$$

The diffusion coefficient has the dimension area/time. We can rewrite Equation 9.7 in a form that shows the temperature dependence for diffusion and a minimum energy for migration to occur:

$$D = D_o \exp(-E^*/RT) \qquad \text{Eq. 9.8}$$

where D_o is a material constant for diffusion that is empirically determined, E^* is the activation energy for migration (kJ/mol), R is the gas constant (8.31 J/mol · K), and T is absolute temperature (in K).[5] We present diffusivity in this particular form, because it is easy to compare with the constitutive equations for flow that were given in Chapter 5 and the relationships discussed later in this chapter.

---

[3] Another Albert Einstein (1879–1955) equation.

[4] Strictly speaking these equations are for vacancy movement, and define D_{vac}.

[5] We may also write this equation involving Boltzmann's constant (k), in which case E^* is given in a different form; k and R are related by the equation $R = kN_A$, where N_A is Avogadro's number (6.02×10^{23}mol^{-1}), which gives $k = 1.38 \times 10^{-23}$. Note that "exp(a)" means e^a.

Two types of solid diffusion in crystals are (1) grain-boundary diffusion or Coble creep, and (2) volume diffusion or Nabarro-Herring creep. When mass transfer involves a reactive and transporting fluid phase, the process that is geometrically similar to grain-boundary diffusion is called pressure solution. We will discuss each of these three mechanisms.

9.5.1 Volume Diffusion and Grain-Boundary Diffusion

Given sufficient time, diffusing vacancies reach the surface of the crystal where they disappear. To see how this causes deformation, consider a crystal that is being subjected to a differential stress (Figure 9.20). The vacancies migrate toward the site where stress is greatest and the atoms move to the sides where the stress is least. This results in an overall change in the distribution of mass, producing a change in shape of the crystal. But realize that this occurs without large-scale distortion of the crystal lattice. The diffusion of vacancies can occur through the entire body of a crystal or can be concentrated along a narrow region at its grain boundary (Figure 9.20a); both result in a permanent shape change as shown in Figure 9.20b. These deformation mechanisms are called **volume diffusion** (or **Nabarro-Herring creep**) and **grain-boundary diffusion** (or **Coble creep**), respectively. Thus, in the presence of a non-isotropic stress field we find that diffusion is directional.

Because both Nabarro-Herring creep and Coble creep achieve strain by the diffusion of vacancies, the strain rate for each mechanism is a function of the diffusion coefficients (volume diffusion [D_v] and grain-boundary diffusion [D_b] coefficients respectively), but also of the grain size (d):

$$\dot{e}_{\text{Coble}} \cong D_b/d^2 \qquad \text{Eq. 9.9}$$

$$\dot{e}_{\text{Nabarro-Herring}} \cong D_v/d^3 \qquad \text{Eq. 9.10}$$

These simplified relationships emphasize the critical importance of grain size in diffusional creep: a larger grain size results in a less efficient process, so a lower strain rate.

The activation energy for grain-boundary diffusion (included in D_b) is less than that for volume diffusion (included in D_v), and the grain-size dependence of volume diffusion is larger. Thus, Coble creep is a more efficient process in crustal rocks than Nabarro-Herring creep, so that the latter is restricted to high-temperature regions (e.g., temperatures in the mantle) and/or to materials with very small grain sizes.

9.5.2 Pressure Solution

Pressure solution is a mass transfer process that occurs in natural rocks at temperatures much lower than those for solid diffusion. The process is geometrically similar to grain-boundary diffusion, but involves the presence of a fluid film on grain boundaries. It is important in crustal rocks because material transfer occurs at temperatures well below those required for vacancy diffusion, thanks to a chemically active fluid film that dissolves the crystal. The dissolved ions then move along a chemical gradient that arises from differential solubility in the presence of a differential (non-isotropic) stress to regions of deposition. Recall that fluids do not support shear stresses (Chapter 3), so pressure solution only works if the fluid film is "attached" to the grain boundary by chemical bonds; thus, the fluid does not move, but dissolved atoms do. Areas of high stress, say surfaces perpendicular to the maximum principal stress, exhibit enhanced solubility and the dissolved material is transported to regions under lower stress (surfaces perpendicular to the minimum principal stress). The geometric properties of the process are very similar to our earlier description of grain-boundary diffusion and, indeed, pressure solution produces shape changes like that in Figure 9.20b, except that it occurs at the low temperatures encountered near the Earth's surface. A way to distinguish between these diffusional deformation mechanisms is to

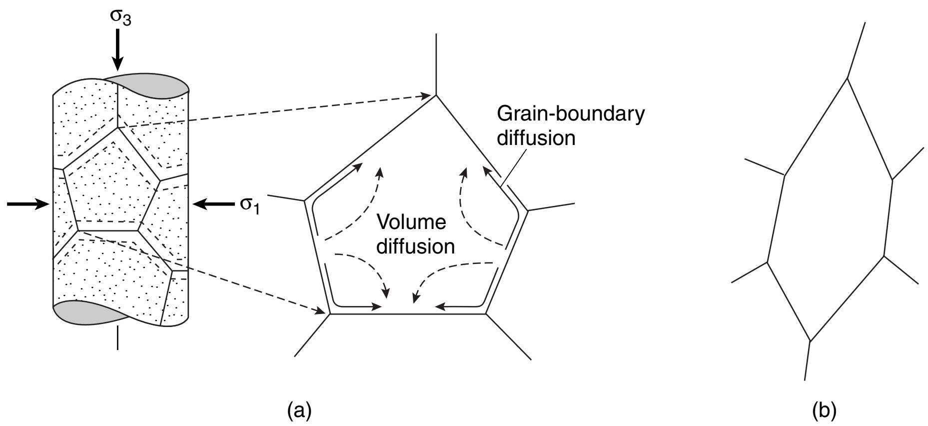

FIGURE 9.20 Diffusional flow by material transport through grains (volume diffusion or Nabarro-Herring creep) and around grains (grain-boundary diffusion or Coble creep), with a differential stress (a) that produces shape change (b).

use the terms **fluid-assisted diffusion** for pressure solution and **solid-state diffusion** for Nabarro-Herring creep and Coble creep; in colloquial terms we sometimes call them "wet diffusion" and "dry diffusion," respectively. Because fluids are abundant in shallow crustal rocks and these have low ambient temperatures, pressure solution is an important deformation mechanism in upper crustal rocks.

We infer the past activity of pressure solution diffusion in rocks from the presence of, for example, stylolites in limestones, grain overgrowths in sandstones, and cleavage and pressure shadows in some slates (Figure 9.21; see also Chapter 11). In contrast to dry diffusion, the distance over which material may be transported by fluid-assisted diffusion is not limited to individual grains, but can be substantial, particularly if the dissolved ions migrate into the pore fluid of the rock. Movement of pore fluid (i.e., groundwater flow) can flush the dissolved ions completely out of the rock, resulting in substantial volume loss. On the mesoscale, pressure solution may result in the formation of alternating layers of different composition, such as quartz-rich and mica-rich layers, in a process called **differentiation** (see Chapter 11). Alternatively, the dissolved ions may precipitate as vein fillings in cracks (Figure 9.21). The widespread occurrence of these pressure-solution structures in natural settings emphasizes the geologic importance of this deformation mechanism.

The strain rate associated with pressure solution is a function of the area and the rate of atoms that go into solution (i.e., the solubility of a material) in the fluid:

$$\dot{e}_{\text{pressure solution}} \cong D_f/d^2 \qquad \text{Eq. 9.11}$$

where D_f is the diffusion coefficient of a phase in a fluid and d is the grain size.

9.6 CONSTITUTIVE EQUATIONS OR FLOW LAWS

We defined the rate at which shape change occurs as the strain rate, $\dot{e}$ (Section 5.1). Since dislocation movement is a function of the differential stress (either arising from internal distortion or externally imposed on the system), the ambient temperature, and the activation energy for breaking bonds, the rate at which strain occurs by dislocation movement is a function of all these parameters. This relationship is described by a **constitutive equation** or **flow law,** with the general form

$$\dot{e} = A\, f(\sigma_d)\, \exp(-E^*/RT) \qquad \text{Eq. 9.12}$$

where A is a material constant, E^* is the activation energy, R is the gas constant, T is the absolute

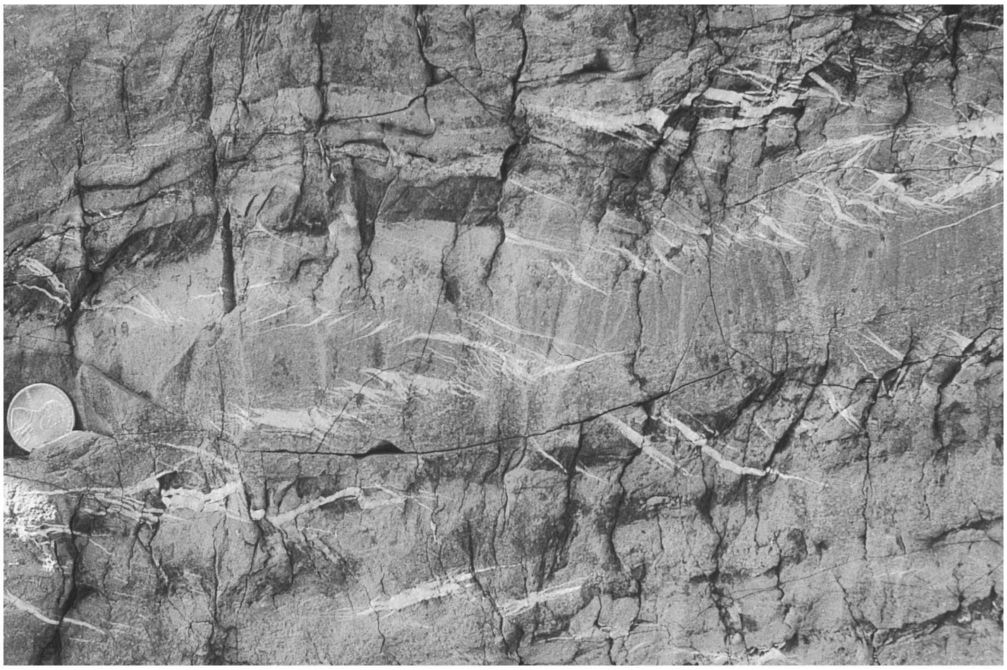

FIGURE 9.21 Bedding-perpendicular pressure solution seams (stylolites) and veins (white structures) in argillaceous limestone (Appalachians, Pennsylvania, USA). The middle bed is pure carbonate and does not contain as many seams. Note that the stylolites cut across bedding.

temperature (in K), and $f(\sigma_d)$ represents a differential stress function; characteristic values for these parameters were given in Table 5.6. In this chapter we focus on the stress function, $f(\sigma_d)$, which is determined from experiments on natural rocks and common minerals. For dislocation glide (low-temperature creep) the function of stress is *exponential,* so the flow law is of the form

$$\dot{e} = A \exp(\sigma_d) \exp(-E^*/RT) \qquad \text{Eq. 9.13}$$

Because of the form of this relationship, dislocation glide is also called **exponential creep.**

For dislocation glide and climb (high-temperature creep), which is typical for deep crustal and mantle rocks, the stress is raised to the *power n.* This flow law takes the general form

$$\dot{e} = A\, \sigma_d^n \exp(-E^*/RT) \qquad \text{Eq. 9.14}$$

Climb-assisted glide is therefore also called **power-law creep,** and the power n is called the *stress exponent.*

In an earlier section we presented the diffusion coefficient for point defects (Equations 9.4–9.6). The motion of individual defects or atoms is similarly a function of differential stress and that has the form

$$\dot{e} = A\, \sigma_d \exp(-E^*/RT)\, d^{-r} \qquad \text{Eq. 9.15}$$

You will notice that the stress function of Equation 9.15 is the same as Equation 9.14, except that the stress exponent, n, equals 1. This means that diffusion is *linearly* related to the strain rate and, therefore, that diffusional creep is a linear viscous process (or Newtonian viscous process; Chapter 5). Note, however, that the strain rate for diffusional creep is nonlinearly related to the grain size, and that the value of r is in the range of 2 to 3 (Equations 9.5, 9.6, and 9.15).

We will see later that these various creep regimes produce characteristic microstructures, but let us revisit the deformation experiments of Chapter 5 and interpret their behavior in light of what we now have learned about defects and crystal plasticity.

9.7 A MICROSTRUCTURAL VIEW OF LABORATORY BEHAVIOR

While our discussion has been pretty theoretical and perhaps esoteric up to this point, it was necessary to understand that defect microstructures can explain how materials respond to stress (i.e., rheology). Deformation experiments typically show the same behavior: after an initial elastic stage, permanent (ductile) strain accumulates. The elastic component is recoverable and does not involve crystal plastic processes, but the ductile component of the curve is mostly achieved by the motion of defects. Strain accumulates at constant stress (steady-state flow), or requires increasingly higher stress (work hardening) at constant $\dot{e}$. From a microstructural perspective, **steady-state flow** implies that the generation, motion and removal of dislocations is sufficiently fast to achieve strain at a constant rate for a certain stress level. But what about a microstructural explanation for **work hardening** (Section 5.4)? Limited climb and cross-slip at low temperatures prevent dislocations from slipping past inclusions and other obstacles. Combined with a decreased frequency of dislocation annihilation, this causes dislocation density in a crystal to increase, which affects the ability of dislocations to glide because they interact with one another. Recall that the ability of dislocations to glide produces strain, so dislocation tangles restrict their motion and the rate of strain accumulation decreases (unless the differential stress increases).

With so many dislocations in a crystal, the chance of interaction is large, so let's look at this in some detail. Figure 9.22 shows a situation where one edge dislocation (D_1) moves relative to an edge dislocation (D_2) with a different slip plane (we keep dislocation D_2 stationary for the convenience of illustrating our point). As D_1 passes through D_2, the dislocation line $\mathbf{l}_2$ is offset (Figure 9.22b). This offset, called a **jog,** has an important implication. Whereas the Burgers vector $\mathbf{b}_2$ for dislocation D_2 remains the same along the dislocation line, its glide plane has changed at the jog. Motion of dislocation D_2 needs a critical resolved shear stress (CRSS) that allows glide on the initial slip plane, but it also needs movement on a second slip plane for that dislocation. Because the values of the CRSS differ for crystal planes in different orientation, the ability for glide varies along the dislocation line when a jog is present, resulting in a dislocation that is held back at the jog (Figure 9.22c). This reduced ability of a dislocation to move is what causes the material to strengthen, expressed as work hardening in experiments. Diffusion of vacancies to segments of the dislocation can overcome the restriction, so work hardening is much less important in the high-temperature creep regime. Thus, the presence of impurities that pin dislocations or high dislocation densities that restrict

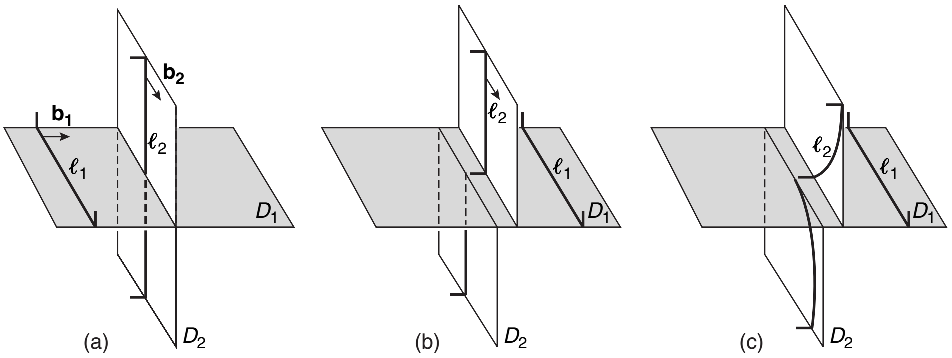

FIGURE 9.22 The formation of a jog from the interaction of two mobile edge dislocations. For simplicity, dislocation D_2 is initially kept stationary while dislocation D_1 moves; the glide planes (shaded and unshaded), Burgers vectors (**b**), and dislocation lines (**l**) for each edge dislocation are shown (a). As D_1 passes through dislocation line $\mathbf{l}_2$, a small step of one Burgers vector ($\mathbf{b}_1$) length is created; this small step is a jog, with a differently oriented dislocation line segment but the same $\mathbf{b}_2$ (b). As a consequence, the glide plane, containing $\mathbf{l}_2$ and $\mathbf{b}_2$, is different along $\mathbf{l}_2$. In fact, the glide plane of the jog is the same of that for D_1, but with a different Burgers vector. Assuming that the CRSS for glide differs in different directions, the ability of D_2 to move is no longer the same along $\mathbf{l}_2$, and the jog pins the dislocation by anchoring a segment of $\mathbf{l}_2$ (c).

dislocation motion (tangles) result in work hardening of materials, which is overcome by the activity of dislocation climb. We also observe *work softening* in some experiments (Section 5.4), but we wait until Section 9.9, where we discuss grain-size reduction, to offer an explanation.

9.8 IMAGING DISLOCATIONS

The dislocation density of an unstrained crystal is on the order of 10^6 cm^{-2} and this value is orders of magnitude higher in strained crystals. A 1 cm^3 volume of a strained quartz crystal with a dislocation density of 10^9 cm^{-2} will have a total dislocation line length of 10^9 cm or 10,000 km (the distance from Earth's equator to pole). Obviously, dislocations and other defects must be quite small to fit so many in a volume that small. We therefore need very large magnifications to see them, and this generally involves transmission electron microscopy (TEM). This technique permits imaging of microstructures at magnifications of up to 500,000×, with a resolution of better than 1 nm (1 nanometer = 10^{-9} m). Such high resolution is not usually necessary for the examination of defect microstructures and more conventional TEM work is done at magnifications of 10,000–100,000× (Figure 9.23). TEM samples require sufficient thinning of the material that it is transparent to the electron beam; generally the thickness of the thin foil is a few hundred nanometers. Crystal defects in thin foils are revealed by diffraction contrasts that result from lattice distortions surrounding the defect, which allows us to determine both the Burgers vector of a dislocation and the crystallographic orientation of the dislocation line (Figure 9.23). Once these are established, it is possible to determine the nature of a dislocation (i.e., whether edge, screw, or mixed) from the angular relationship between **b** and **l.** Recall that for edge dislocations **b** and **l** are perpendicular, and for screw dislocations **b** and **l** are parallel.

In Figure 9.9 we observed dislocation clusters in olivine using the standard petrographic microscope and a decoration technique. Individual dislocation geometries in olivine in the transmission electron micrograph were shown in Figure 9.5, where we can distinguish arrays of parallel dislocations (lower right), straight dislocations (upper half), and dislocation loops (lower left). The terminations of the dislocations in this photomicrograph arise from the intersection of the dislocation line with the lower and upper boundaries of the thin foil; the thicker the foil the longer the dislocation would appear, until it intersects the crystal edge. Note the geometric similarity between the optical and transmission electron micrographs of Figures 9.5 and 9.23, which both contain straight dislocation lines with sharp angular bends as predicted by slip systems in olivine (Table 9.1).

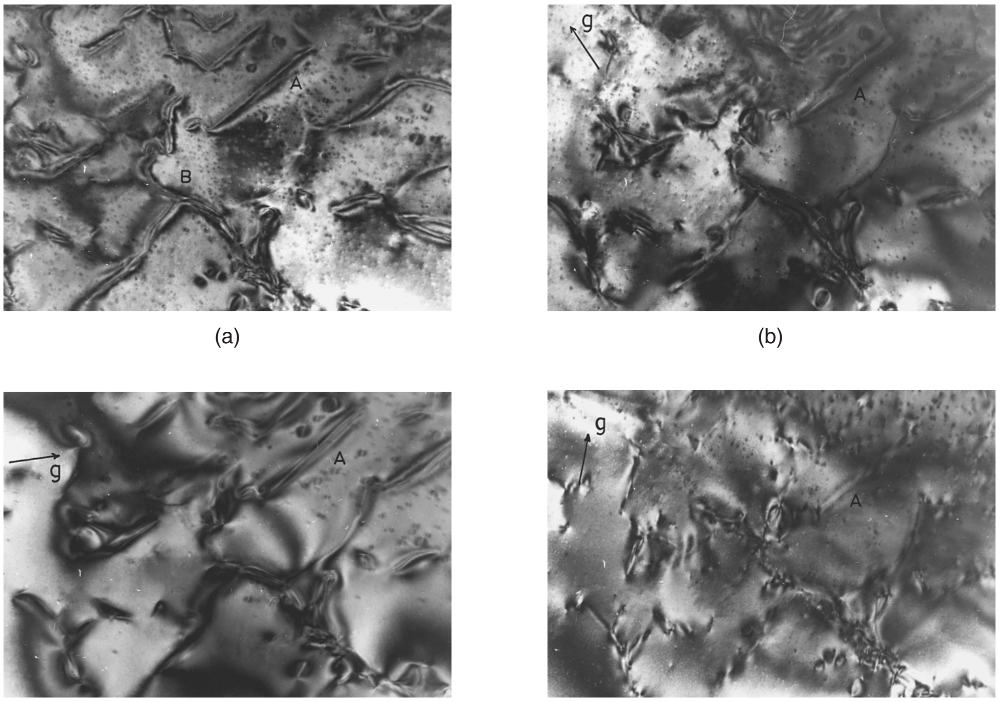

(a) (b) (c) (d)

FIGURE 9.23 Dislocations in calcite (a) and determination of the Burgers vector using transmission electron microscopy (TEM). View of the same area for different diffracting lattice planes: (b) (0006), (c) (10$\bar{1}\bar{2}$), (d) (10$\bar{1}$4); the orientation of the lattice plane in each image is indicated by its pole (marked by vector **g**). The presence of dislocation *A* in (b) and (c) rules out all possible Burgers vectors in calcite with the exception of <$\bar{2}$021>; this is confirmed by the absence of contrast from dislocation *A* in (d). This (time-consuming) procedure is called the *invisibility criterion.* The Burgers vector is neither exactly perpendicular nor parallel to the dislocation line, so dislocation *A* is a mixed dislocation. Width of view of each TEM image is ~1.7 μm.

9.9 DEFORMATION MICROSTRUCTURES

Can we recognize the (past) activity of a particular deformation mechanism and, by inference, determine the rheologic conditions during deformation? The answer to this question is mostly yes, because deformation mechanisms produce relatively characteristic microstructures that can be observed in hand specimens and thin section. However, a rock's "memory" can be incomplete; only the latest deformation mechanism may be preserved. Once we establish the operative deformation mechanism from microstructures we can proceed to make predictions about the conditions of temperature, stress, and strain rate during deformation, which is the ultimate reason to study microstructures. Throughout the book we use the term **microstructure** to describe geometric characteristics of rocks on the scale of the microscope; for example, twins are a microstructural element. We use the term **(micro)fabric,** which means different things to different people, with an appropriate modifier (such as dimensional-preferred fabric for geometric alignments). In Chapter 12 we introduce yet another type of fabric, **crystallographic-preferred fabric,** that describes the degree of crystal lattice orientation of a mineral aggregate.

In the next several pages we look at the characteristic microstructures in deformed rocks that arise from three mechanisms: recovery, recrystallization, and superplastic creep. Mechanical twinning, a fourth mechanism, was discussed earlier (Section 9.5). To assist you with the many new concepts that will be introduced, brief descriptions of the processes, characteristic microstructures, and some related terms of crystal plastic and diffusional creep are given in Table 9.3.

9.9.1 Recovery

The presence of crystal defects such as dislocations and twins increases the **internal strain energy** of a grain, because the crystal lattice surrounding the defects is distorted. The atomic bonds are bent and

TABLE 9.3 SOME TERMS AND CONCEPTS RELATED TO CRYSTAL PLASTICITY AND DIFFUSIONAL CREEP

Annealing	Loosely used term for high-temperature grain adjustments, including static recrystallization and grain growth.
Bulge nucleation	A type of migration recrystallization in which a grain boundary bulges into a grain with higher internal strain energy, forming a recrystallized grain.
Dislocation wall	Concentration of dislocations in a planar array.
Dynamic recrystallization	Formation of relatively low-strain grains under an applied differential stress.
Foam structure	Recrystallized grain structure characterized by the presence of energetically favorable grain-boundary triple junction (at ≈120° angles).
High-angle boundary	Boundary across which the crystallographic mismatch exceeds 10°; characteristic of recrystallization.
Low-angle boundary	Tilt boundary across which the crystallographic mismatch is less than 10°; characteristic of recovery.
Migration recrystallization	Recrystallization mechanism by which grain boundaries move driven by a contrast in strain energy between neighboring grains.
Polygonized microstructure	Recovery structure showing elongate to blocky subgrains (mostly used for phyllosilicates).
Recovery	Process that forms low-angle grain boundaries by the temperature-activated rearrangement of dislocations.
Recrystallization	Mechanism that removes internal strain energy of grains remaining after recovery, producing high-angle grain boundaries that separate relatively strain-free (recrystallized) grains.
Recrystallized grains	Relatively low-strain grains that are formed by recrystallization.
Rotation recrystallization	Recrystallization mechanism by which dislocations pile up in a tilt boundary, thereby “rotating” the crystal lattice of the area that is enclosed by the tilt boundary.
Static recrystallization	Formation of strain-free grains after deformation has stopped (i.e., differential stress is removed).
Subgrain	Area of crystallographic mismatch that is less than 10° relative to the host grain.
Subgrain rotation	Rotation recrystallization mechanism by which dislocations continue to move into a low-angle tilt boundary surrounding a subgrain, thereby increasing the crystallographic mismatch and forming a high-angle grain boundary.
Superplastic creep	Grain-size-sensitive deformation mechanism by which grains are able to slide past one another without friction because of the activity of diffusion (as opposed to frictional sliding or cataclasis).
Tilt boundary	Concentration of dislocations in a planar array.
Twinning	Deformation mechanism that rotates the crystal lattice over a discreet angle such that the twin boundary becomes a crystallographic mirror plane. Such a planar defect is produced by the motion of partial dislocations.
Undulose extinction	Irregular distribution of dislocations in a grain, producing small crystallographic mismatches or lattice bending that is visible under crossed polarizers.

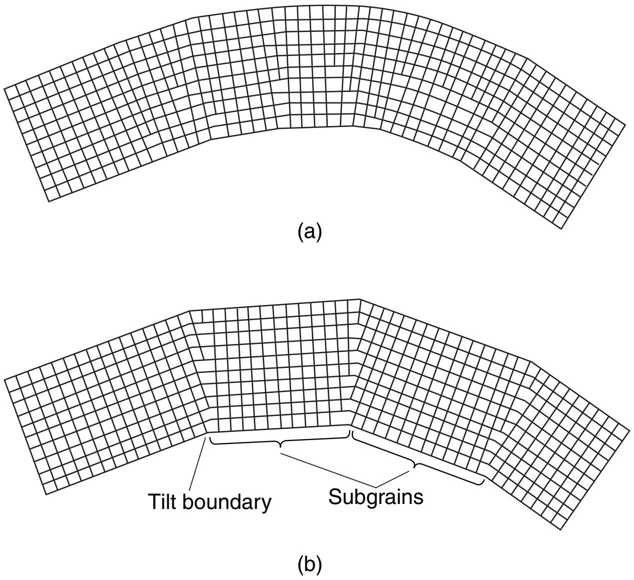

FIGURE 9.24 Irregularly distributed dislocations (a) are rearranged by glide and climb to form a dislocation wall (or tilt boundary) that separates subgrains (b).

stretched (to give the "strain" in strain energy), so that the crystal lattice is not in its lowest energy state. Dislocation creep lowers the internal strain energy by annihilation and/or moving dislocations to the edge of crystals, so that the internal strain is minimized. This is the reason that internal strain energy is also called the **stored strain energy.** However, this does not mean that internal strain is recoverable (as in elastic strain), because permanent distortions are produced around dislocations in the crystal (recall Figure 9.12). Another way to change the internal strain energy of a grain is by localization of crystal defects. As a result of climb, cross-slip, and glide, dislocations can be arranged into a zone of dislocations, called a **dislocation wall** or **tilt boundary.** Such tilt boundaries produce a lower strain energy state in most of the grain than when dislocations are more evenly distributed across the grain (Figure 9.24). A single dislocation produces only a small crystallographic distortion that is not visible optically, but an array of dislocations in a tilt boundary makes the crystallographic mismatch optically visible (Figure 9.25). The greater the number of dislocations in the wall, that is, the closer their spacing, the greater the crystallographic mismatch across the boundary. The angular mismatch, θ, across a tilt boundary is a function of the length of the Burgers vector **(b)** of a dislocation and the spacing (*h*) of individual dislocations in the wall

$$2\sin(\theta/2) = \mathbf{b}/h \qquad \text{Eq. 9.16}$$

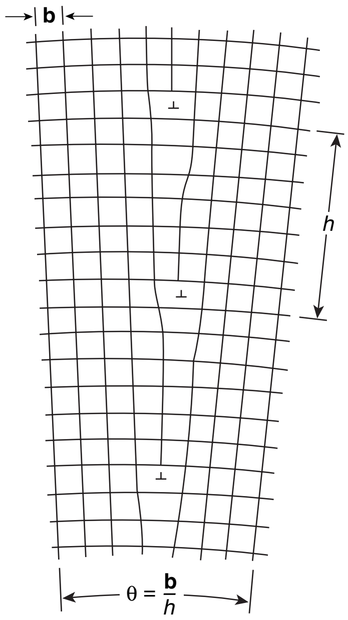

FIGURE 9.25 A tilt boundary composed of edge dislocations at a distance *h* apart in a simple lattice. The crystal lattice across the boundary does not have the same orientation, but is rotated over an angle θ (in radians) = **b**/*h*, where **b** is the Burgers vector and *h* is the spacing of dislocations in the tilt wall.

or for small angles of θ (in radians)

$$\theta = \mathbf{b}/h \qquad \text{Eq. 9.17}$$

We call the region of a large crystal that is enclosed by a low-angle tilt boundary a **subgrain.** The convention to distinguish between low-angle (subgrains) and high-angle boundaries (recrystallized grains; discussed later) is an angular difference across the tilt boundary that is less than 10°. With this information we can estimate the number of dislocations in a tilt wall 500 μm long by 2 nm wide (using Equations 9.16 and 9.17), assuming a Burgers vector of 0.5 nm length and an angular mismatch θ of 10°. This implies that the dislocation spacing is approximately 2.9 nm and thus that there are more than 170,000 (!) dislocations in this low-angle tilt boundary, representing a dislocation density in the area of the low-angle tilt wall (1×10^{-8} cm^2) of 1.7×10^{13} cm^{-2}. This is many orders of magnitude greater than dislocation density in undeformed crystals.

In thin section, especially under cross-polarized light, undulatory extinction is one manifestation of the crystallographic mismatch that produces subgrains. It is particularly common in the minerals calcite, quartz, olivine, and pyroxene (Figure 9.26). **Recovery** is the name of the process forming low-angle grain bound-

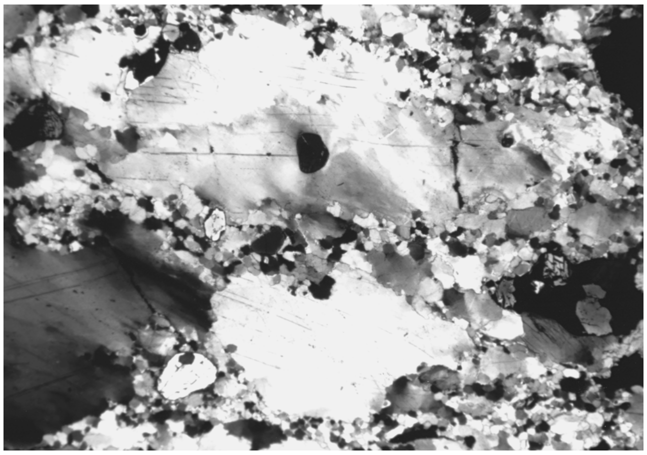

FIGURE 9.26 Subgrain microstructure and undulose extinction in a marble mylonite from southern Ontario (Canada). Width of view is ~4 mm.

aries by the temperature-activated rearrangement of dislocation, which produces the characteristic subgrain deformation microstructure. In the case of phyllosilicates, such as muscovite, these subgrains are also called a **polygonized microstructure,** which describes the archlike geometry where each segment is oriented at a slightly different angle from the next. Experiments in which recovery dominates have shown that the stress function of the associated flow law is exponential (Equation 9.13). Materials scientists, therefore, use the term **exponential-law creep** for recovery microstructures.

9.9.2 Recrystallization

The process removing the internal strain energy that remains in grains after recovery is called **recrystallization;** it forms **high-angle grain boundaries** that separate relatively strain-free grains from each other. In rocks, a recrystallized microstructure is characterized by grains without undulatory extinction and with relatively straight grain boundaries that meet at angles of about 120° (Figure 9.27). Another example of this process and the resulting structure is found in the foam of soap. Looking closely at foam while doing the dishes or washing your hair, you will see all the geometric characteristics of a recrystallized microstructure. Because some of the same energy considerations are involved in the structure of foam,[6] we also call the microstructure of recrystallized rock a **foam structure.**

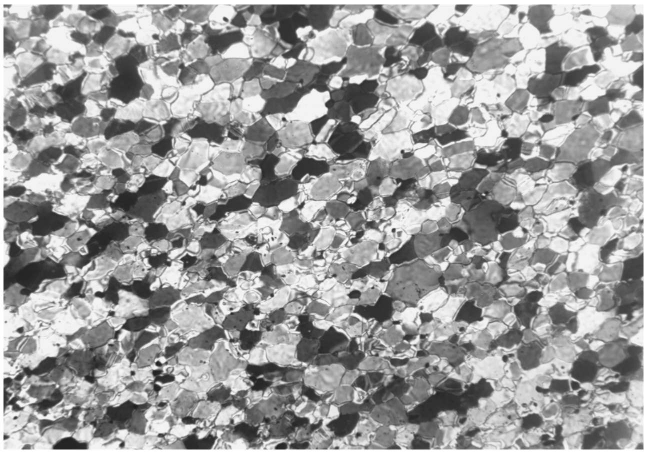

FIGURE 9.27 Recrystallization microstructure, showing relatively strain-free grains with straight grain boundaries. This image represents the most deformed stage in a marble mylonite that is also shown in Figures 9.15 and 9.26 (Ontario, Canada). Width of view is ~2 mm.

FIGURE 9.28 Microstructure of a mylonite. Note the fine-grained, quartz-rich matrix that surrounds relatively rigid feldspar clasts. Width of view is ~1 cm.

Recrystallization within an anisotropic stress field (i.e., a differential stress) is called **dynamic recrystallization.** Dynamic recrystallization results in grain-size reduction, which is well known from sheared rocks (such as mylonites; Figure 9.28). We return in more detail to mylonites in Chapter 12, but at this point we note that they have a grain size that is smaller than that of the host rock from which they formed. In fact, the term mylonite is unfortunate for these microstructures as it derives from the Greek word "mylos," meaning milling. At the time of their discovery in northern Scotland by Sir Charles Lapworth in the late 1900s (Chapter 12) it was thought that they were formed by a grinding process (which we now call cataclasis).

---

[6] In foam, however, surface energy dominates, whereas internal strain energy is more important in deformed rocks.

Since their original discovery we have learned that this is incorrect, and that dynamic recrystallization is responsible for grain-size reduction; nonetheless, the name mylonite has persisted. Based on experimental work, dynamic recrystallization can be used as a semi-quantitative indicator of the temperature conditions during deformation; for example, recrystallization begins at ~300°C for calcite, ~350°C for quartz, and ~450°C for feldspar. These estimates seem to agree well with temperature estimates in deformed natural rocks.

Recrystallization occurring under isotropic stress conditions or when the differential stress is removed is called **static recrystallization;** otherwise know as **annealing.** From a microstructural perspective the only thing that distinguishes static recrystallization from dynamic recrystallization is a relatively larger recrystallized grain size. Static recrystallization reduces the internal strain energy by the formation of relatively large, strain-free grains that grow to decrease the total free energy of the rock.[7]

A closing comment about the use of the term recrystallization before we turn to the operative mechanisms. Recrystallization as used here involves changes in the strain energy of a *single phase,* whereas the term recrystallization in petrology involves multiple *phases.* In petrology the process is governed by chemical potentials rather than by strain potentials. Be sure not to confuse these very different meanings of the term recrystallization.

9.9.3 Mechanisms of Recrystallization

There are two main mechanisms for recrystallization: (1) rotation recrystallization and (2) migration recrystallization. **Rotation recrystallization** describes the progressive misorientation of a subgrain as more dislocations move into the tilt boundary, thereby increasing the crystallographic mismatch across this boundary. This produces a high-angle grain boundary without appreciable migration of the original (sub)grain boundary (Figure 9.29a). Eventually the crystallographic mismatch is sufficiently large that individual grains are recognized. Remember that progressive rotation of the subgrain occurs only by adding more dislocations in the boundary and that there is never loss of cohesion with the crystal lattice of the host grain. The convention we previously introduced to distinguish subgrains (low-angle grain boundaries) from recrystallized grains (high-angle grain boundaries) is an angle of 10°. This is admittedly an arbitrary convention, as we find a progression from low-angle to high-angle grain boundaries in rocks, but it is convenient for our purposes. Recrystallized grains are best

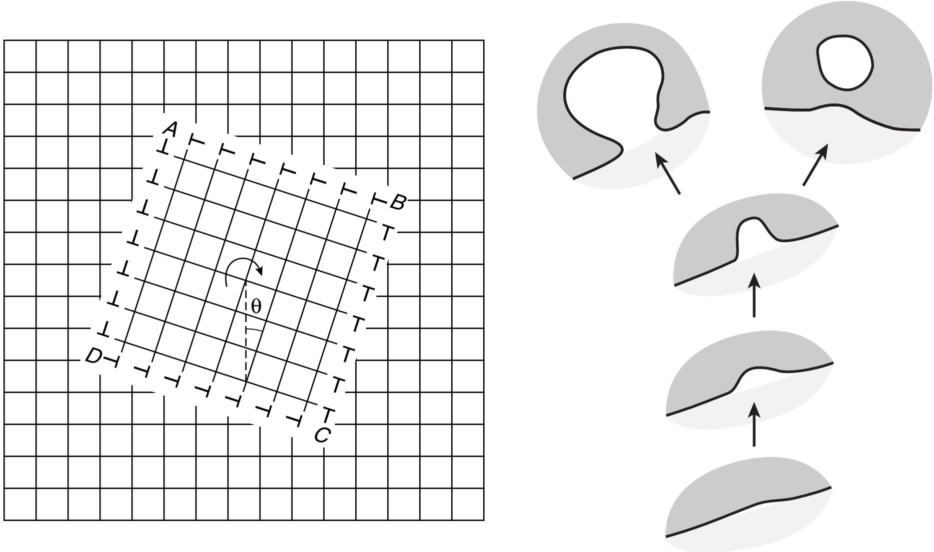

(a) (b)

FIGURE 9.29 Recrystallization by (a) subgrain rotation and (b) bulge nucleation. In (a), a portion of a crystal is bounded by four tilt boundaries (*ABCD*); rotation by adding more dislocations of the same sign leads to a progressively greater misorientation (i.e., a recrystallized grain). In (b), growth of a dynamically recrystallized grain occurs by bulge nucleation of the grain boundary into a neighboring grain with higher internal strain energy (dark gray), leaving behind a relatively strain-free region that eventually develops into a recrystallized grain.

---

[7] This is sometimes called *secondary* or *exaggerated grain growth.*

developed where large strain gradients exist, such as at grain boundaries. The common microstructure in which relatively deformation-free grain interiors progress to subgrains and then to recrystallized grains toward grain boundaries (Figure 9.30) is called a **core-mantle structure** or **mortar structure.** Rotation recrystallization has been observed in most common rock-forming minerals, including calcite, quartz, halite, and olivine.

Migration recrystallization is a process by which grains grow at the expense of their neighbor(s)—when grain boundaries effectively sweep through neighbors. The grain that grows has a lower dislocation density than the grain(s) consumed. Let's look at an example where the boundary of grain *A* migrates into grain *B* (Figure 9.29b). Keep in mind that a grain boundary separates two crystals whose lattices are not parallel. Migration happens when atoms in grain *B* near the boundary rearrange so they fit into the lattice of the crystal with lower dislocation density (grain *A*). As soon as this happens, these atoms become part of grain *A*. It is easier to rearrange atoms and bonds in grain *B* that are stretched and misoriented, because of its higher dislocation density. As the grain with lower dislocation density grows at the expense of the grain with higher dislocation density, the internal strain energy of the overall system decreases. Typically the boundary of the grain with lower dislocation density bulges into the grain with higher dislocation density (Figure 9.29b). Thus, this recrystallization process has been called **bulge nucleation.** When new grains deform as they grow, this may eventually arrest their growth. In natural settings, quartz, halite, and feldspar commonly recrystallize by bulge nucleation.

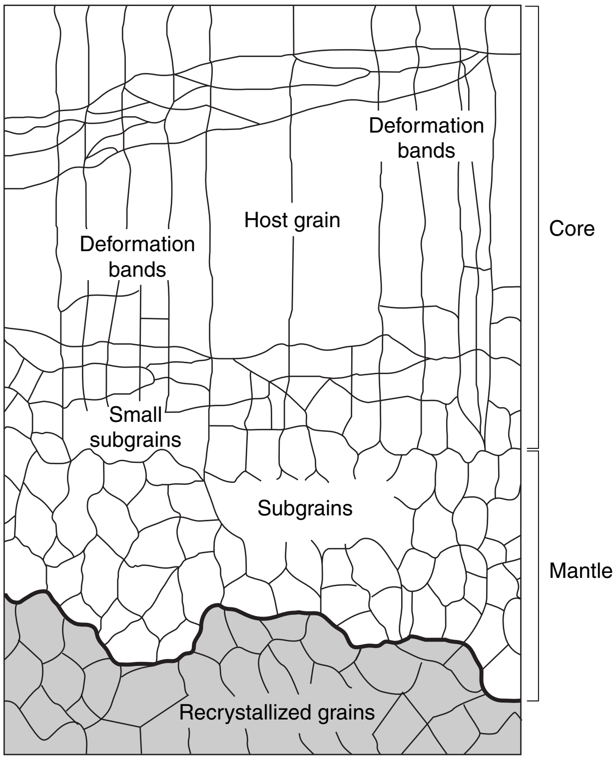

FIGURE 9.30 Core-mantle microstructure (or mortar structure). Recrystallized grains occur at the edge of the mantle by progressive misorientation of subgrains. The internal portion of the host grain (core) shows weak deformation features such as undulose extinction and deformation bands, or may even be strain-free.

The dominance of rotation recrystallization (subgrain rotation) and migration recrystallization (bulge nucleation) is largely a function of strain rate. Consider this: If you are in a hurry to get somewhere, you will try to take the fastest means of transportation. Similarly, nature uses the mechanism that produces the highest strain rate to reduce the internal strain energy of the system. Bulge nucleation is generally favored at higher strain rates and high temperatures. For both recrystallization mechanisms, the recrystallized grain size is inversely proportional to the strain rate. The smaller recrystallized grain size in mylonitic rocks, for example, is indicative of strain-rate increase. We observed **work softening,** strain-rate increase at constant stress, in some experiments (Chapter 5), which can now be understood in terms of the role of grain-size reduction during deformation.

The formation of recrystallized grains is driven by the generation and motion of dislocations, which in turn is driven by differential stress. One may, therefore, expect that a relationship exists between recrystallized grain size and differential stress magnitude. Indeed, experiments have shown that a characteristic range of grain sizes occur for a specific condition of stress and mechanism of recrystallization. This means that we can potentially estimate paleostress conditions from microstructures; that is, recrystallized grain size can be used as a **paleopiezometer** (derived from the Greek "piezo," meaning to press).[8] This is potentially a very powerful tool for understanding deformation, because paleostress is a notoriously difficult parameter to extract from rocks. Although the debate about the exact relationship is not settled, it is generally agreed that recrystallized grain size is inversely proportional to differential stress magnitude

$$\sigma_d = Ad^{-i} \qquad \text{Eq. 9.18}$$

where *A* and *i* are empirically derived parameters for a mineral and *d* is grain size in micrometers (μm). To

---

[8] Piezometers using free dislocation density and subgrain size also exist, but these data are more difficult to obtain and the methods appear less reliable.

TABLE 9.4 **EMPIRICALLY DERIVED PARAMETERS FOR RECRYSTALLIZED GRAIN SIZE–DIFFERENTIAL STRESS RELATIONSHIPS**

Mineral	*A* (in MPa)	*i* (with *d* in µm)
Calcite	467	1.01
Quartz	381	0.71
Quartz ("wet")	4090	1.11
Olivine	4808	0.79

Sources: Mercier et al. (1977), Ross et al. (1980), Schmid et al. (1980), Ord and Christie (1984).

give you a rough idea of these relationships, we list representative parameters for three common minerals, calcite, quartz, and olivine, in Table 9.4. These data are plotted in Figure 9.31, showing representative stress values. In considering these values, remember that considerable uncertainty surrounds paleopiezometry.

Overall, a small recrystallized grain size in a deformed rock reflects a high strain rate, a high differential stress magnitude, or a combination of both. Rock experiments show that the corresponding stress function during recrystallization has the form $f(\sigma) = \sigma^n$ (Equation 9.14), so it is also called **power-lap creep.** The value of *n,* the **stress exponent,** varies, but typically lies in the range of 2 to 5 for common monomineralic rocks (see Table 5.6).

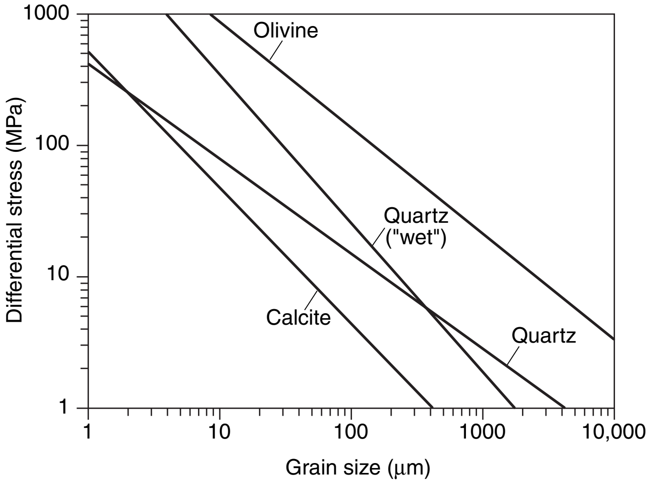

FIGURE 9.31 Empirically derived recrystallized grain size versus differential stress relationships for calcite, quartz, "wet" quartz, and olivine, using the parameters listed in Table 9.4. Note that we plot log σ_b versus log *d,* so that small shifts in the position of each curve reflect large changes in ambient conditions.

9.9.4 Superplastic Creep

Superplastic creep, more completely described by the somewhat cumbersome name **grain-boundary sliding superplasticity (GBSS),** will at first seem out of place after a discussion of dislocation creep mechanisms, because it returns us to the topic of diffusion. This mechanism is intentionally kept to the last, because it occurs at the highest temperature conditions. We look at the characteristics first. Superplastic creep is a grain-size-sensitive deformation mechanism in which grains change shape so they can slide past one another. This sounds like cataclastic flow, but there is an important distinction: in superplastic creep, volume and grain-boundary diffusion are sufficiently efficient to keep gaps from forming between moving grains, and therefore grains are able to slide *without friction.* Strain is produced by neighbor switching as illustrated in Figure 9.32. Superplastic creep can result in very large strains (>1000%) without appreciable internal deformation of the grains. The original definition of superplasticity is, in fact, this ability of rocks to accumulate very large strains without mesoscopic breaking. Even after large finite strains, grains are equiaxial and "fresh-looking," and show no preferred elongation or crystallographic fabric. This diffusion-assisted mechanism is mainly important in materials with relatively small grain sizes (<15 µm) that facilitate diffusion. In this context, recall Equations 9.9 and 9.10, which show the inverse exponential proportionality of diffusion to grain size.

Superplastic creep has been proposed as a natural deformation mechanism in fine-grained calcite- and quartz-rich rocks. The very high temperatures that occur in the (upper) mantle may also permit this mechanism in coarser-grained olivine-rich rocks. Superplastic creep is possible at lower differential stresses than dislocation creep, but requires rocks with relatively small grain sizes. Thus, a rock may initially deform by dynamic recrystallization until its grain size is sufficiently reduced for superplastic creep to occur. When this happens, the rock becomes much weaker; that is, the stress necessary to produce strain decreases. This weakening, known as work or strain softening, is common in ductile fault zones.

The stress function of the flow law for superplasticity approaches linearity between strain rate and stress; that is, the stress component *n* of Equation 9.15 approaches 1. Consequently, the strain rate is inversely proportional to grain size

$$\dot{e} \cong d^{-r}$$

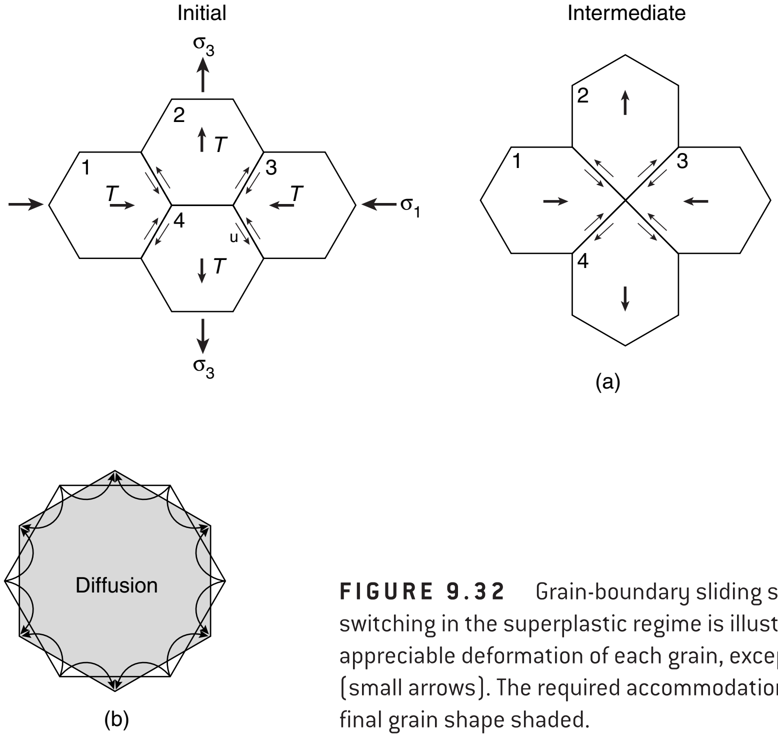

(a)

(b)

FIGURE 9.32 Grain-boundary sliding superplasticity (or superplastic creep). In (a), neighbor switching in the superplastic regime is illustrated. A group of four grains enjoy ~55% strain without appreciable deformation of each grain, except at the boundaries to accommodate grain sliding (small arrows). The required accommodation of local strain by diffusion is shown in (b), with the final grain shape shaded.

where r is 2 to 3 based on experimental work. Recalling that a linear relationship between strain rate and stress defines linear viscous rheology (Chapter 5), superplastic creep is well described by Newtonian fluid mechanics. This contrasts with dislocation creep, which typically has nonlinear rheology ($n \neq 1$). To emphasize this strong grain-size dependence of superplastic creep we also call it **grain-size-sensitive creep.**

9.10 DEFORMATION MECHANISM MAPS

Quite an array of concepts and terms have by now been introduced, so let's attempt to create, out of this information, a pattern that helps you to remember the important elements and relationships. The activity of ductile deformation mechanisms can be summarized in a diagram that shows over what ranges of stress, strain rate, temperature, and grain size each mechanism dominates for a given material; such diagrams are called **deformation mechanism maps.**[9] The variables may be stress (e.g., differential stress), temperature, and grain size, but for comparison between different materials we generally use normalized parameters. A normalized physical quantity is the ratio between a variable and a material constant measured in the same units. In this case, stress is normalized to an elastic modulus of the material (typically the shear modulus, G), and temperature (absolute temperature, in K) is normalized to the absolute melting temperature of the material (Figure 9.33), called the homologous temperature, T_h. On

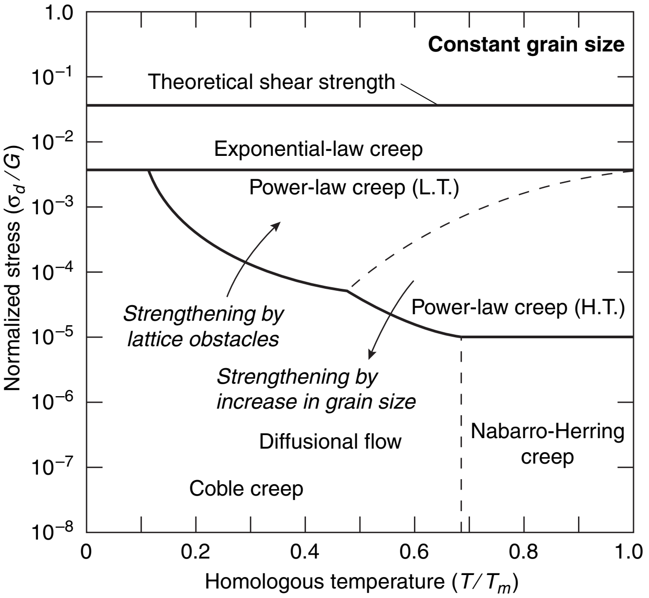

FIGURE 9.33 Schematic of a deformation mechanism map, showing normalized stress versus homologous temperature at a constant grain size.

---

[9] Also called Ashby diagrams, after the British material scientist Michael Ashby who proposed the construction in the early 1970s.

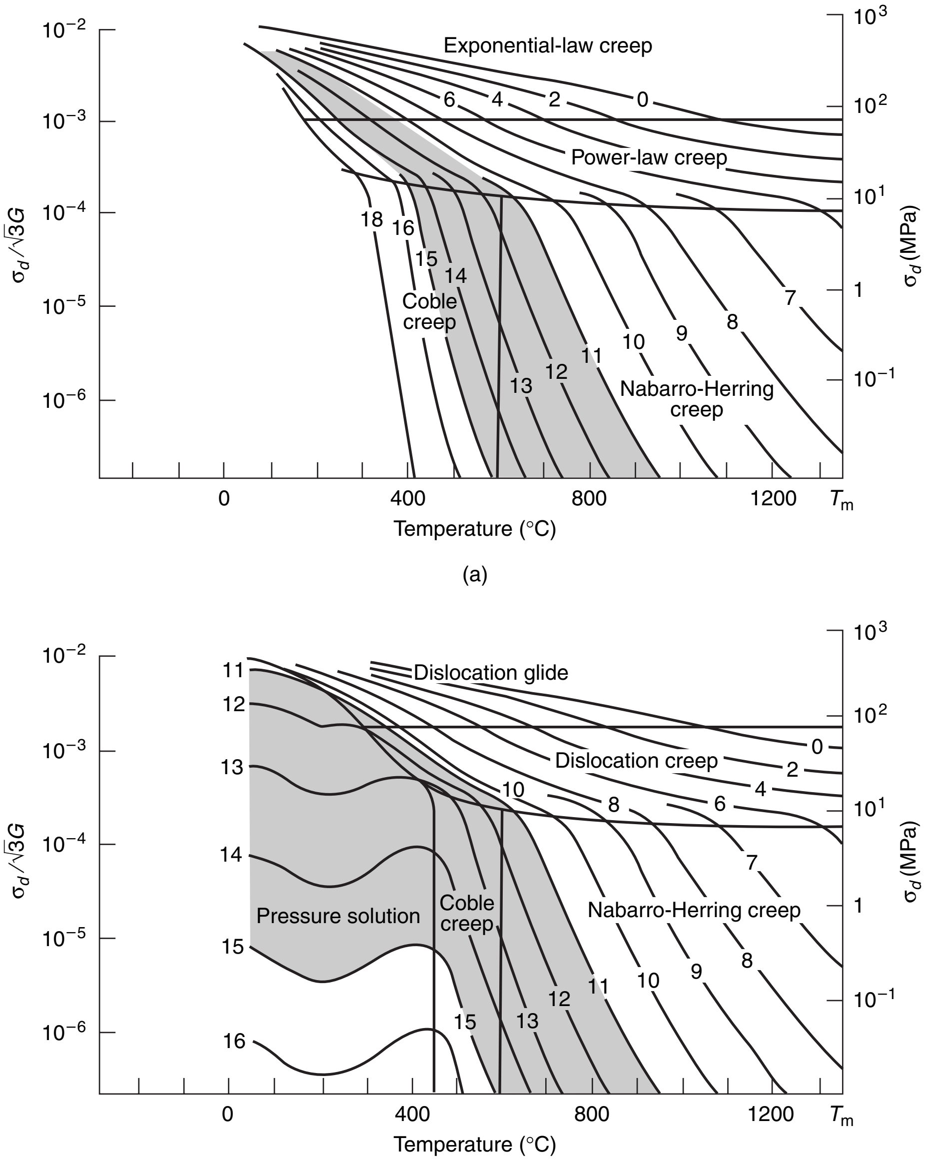

FIGURE 9.34 Deformation mechanism maps for calcite (a) without and (b) with a pressure solution field for a grain size of 100 μm. Contours of –log strain rate are shown; σ_d is differential stress; G is shear modulus; the σ_d-scale on the right is for a shear modulus, G, at 500°C. The undulation of strain rate contours in the pressure solution field arises from the competition between change in the solubility of calcite and fluid concentration with pressure as temperature increases. The range of reasonable geologic strain rates (10^{-11}–10^{-15}/s) is shaded.

the deformation mechanism map we display lines of constant strain rate, as shown in Figures 9.34 and 9.35. Only a small region of the diagram can be constrained by laboratory experiments, so we must extrapolate to most natural conditions. This is comparatively easy where an essentially linear (Newtonian) relationship exists between $\dot{e}$ and σ, such as for diffusional flow. For other regimes, such as dislocation glide (exponential-law creep), and dislocation glide and climb (power-law creep), the extrapolation of these nonlinear relationships is more tenuous. Figures 9.34a and 9.35a show examples of deformation mechanism maps for two common crustal minerals, calcite and quartz, while in Figures 9.34b and 9.35b the pressure solution fields (“wet” diffusion) have been added.

The meaning of boundaries between the fields on a deformation mechanism map is not straightforward, because deformation mechanisms do not change abruptly at this boundary; rather, several mechanisms operate simultaneously. The mechanism that generates

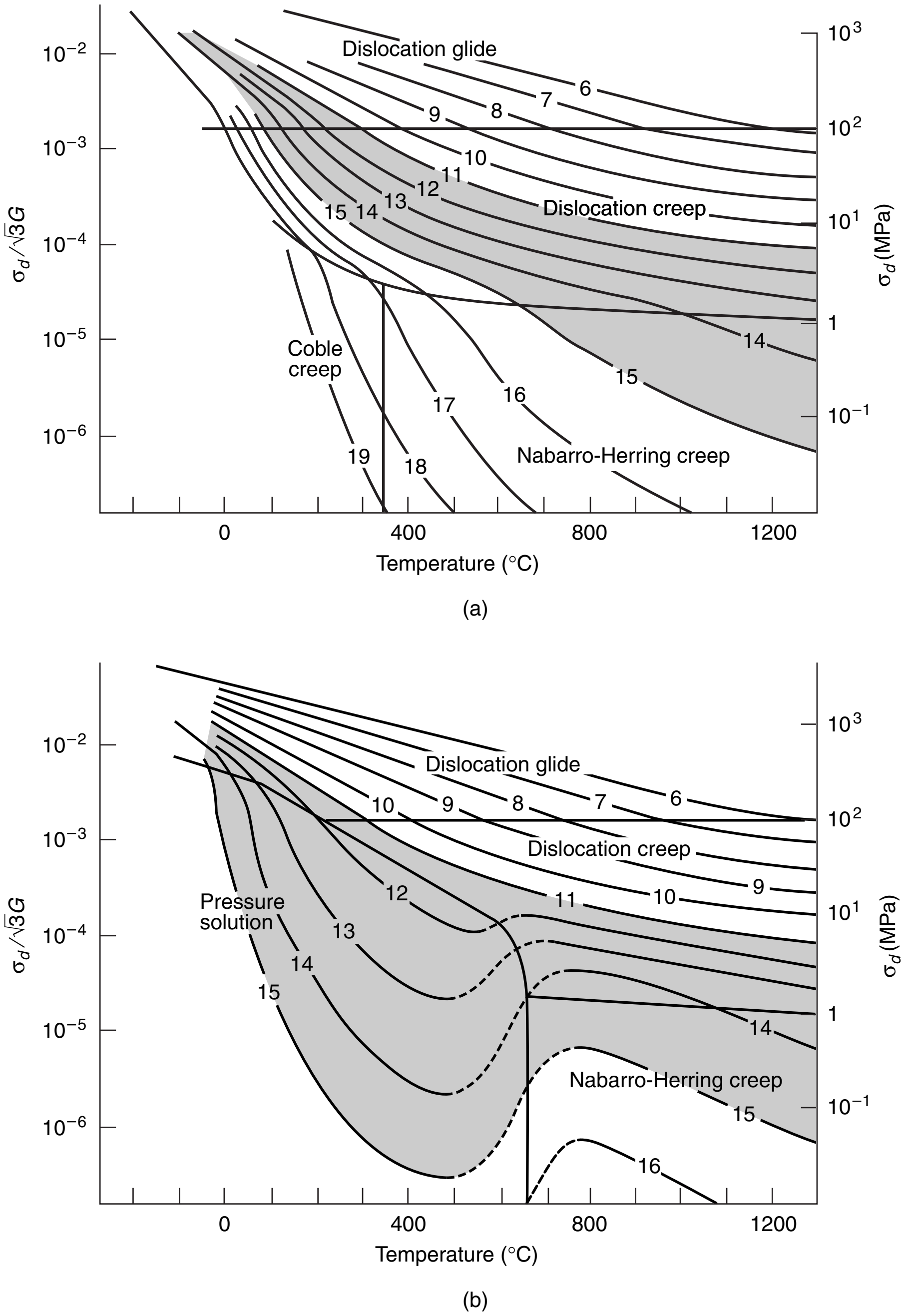

FIGURE 9.35 Deformation mechanism map for quartz (a) without and (b) with a pressure solution field for a grain size of 100 μm. Contours of –log strain rate are shown; σ_d is differential stress; G is shear modulus; the σ_d-scale on the right is for a shear modulus, G, at 900°C. The stress exponent, n, in the power-law field is 4. The region of dashed strain-rate contours represents the inhibition of pressure solution through decrease in pore water concentration.

the highest strain rate is the dominant deformation mechanism. Fields in deformation mechanism maps are defined by calculating the strain rate for each mechanism. Then, the mechanism giving the fastest rate is taken as representative for a field (i.e., the mechanism dominating flow). For example, the field for dislocation creep represents the range of conditions for which dislocation glide creates a strain rate faster than any other mechanism, even though such other mechanisms may be operating. This means that at a boundary the two adjacent deformation mechanisms are equally important.[10] Let's give a practical example. During

---

[10] To emphasize this aspect, deformation mechanism maps are also called *deformation regime maps.*

mylonitization of a quartzite, dynamic recrystallization may dominate; yet diffusional flow may occur simultaneously if the grain size and the strain rate are sufficiently small. Consequently, the map will indicate that we are in the power-law field, but we also see microstructural evidence for diffusional flow.

A general pattern is common to all deformation mechanism maps, which we illustrate with the mineral olivine (Figure 9.36). Instead of homologous temperature we plot depth in Earth, based on a thermal gradient that exponentially decreases from 300K at the surface to 1850K at a depth of 500 km. This enables us also to take into account any effects of pressure, which play a role in the mantle by increasing the flow strength and decreasing the strain rate. From the olivine deformation mechanism map you see that cataclastic flow and exponential-law creep are restricted to relatively large differential stresses (here ≈ 8×10^2 MPa), meaning that these mechanisms are limited to shallow crustal levels. With depth, we pass from exponential-law creep to power-law creep to diffusional creep, given a constant geologic strain rate (say, 10^{-14}/s). In the latter regime, we may pass from grain-boundary diffusion (Coble creep) to volume diffusion (Nabarro-Herring creep), given further temperature or strain-rate change.

The value of a deformation mechanism map lies in its ability to predict the mechanism that dominates a flow under natural conditions. For example, if we assume that the Earth's upper mantle consists mainly of olivine, we predict that at strain rates greater than 10^{-11}/s dislocation glide and climb dominate flow in the upper 100 km, given a grain size of 100 μm. If the strain rate is less, diffusional creep will be more important, especially if the grain size is small. The latter point, the effect of grain size, may not be clear from any of the deformation mechanism maps shown thus far, because grain size was taken as constant value. So how do we know the role of grain-size variation? Consider the flow laws for diffusional creep (Equation 9.15), which state that strain rate is inversely proportional to the square or cube of the grain size. Reducing grain size by, say, one order of magnitude will increase strain rate by two to three orders of magnitude, which will move the field of reasonable geologic strain rates into the regime of diffusional flow. Similarly, if we construct a map for a grain size of, say, 1 mm (1000 μm) or larger, the field of geologic strain rates moves into the regime of power-law creep. With grain sizes for upper-mantle olivine in the range of 100–1000 μm, the microstructures of mantle rocks generally support the predictions that we obtain from olivine deformation-mechanism maps.

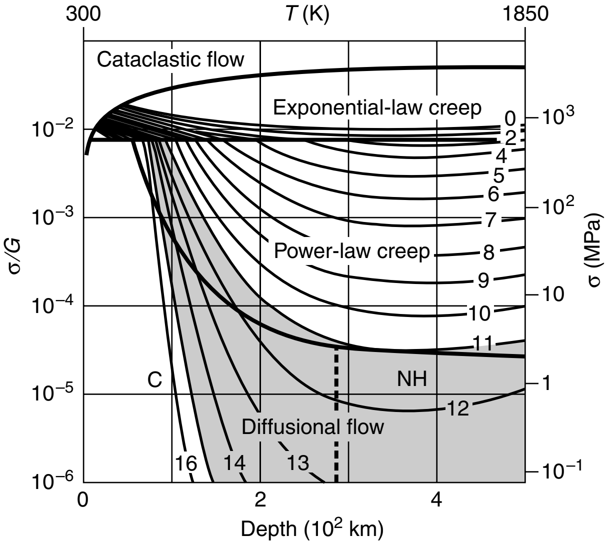

FIGURE 9.36 Deformation mechanism map for olivine with a grain size of 100 μm. Variables are the same as in Figure 9.33, except that depth is substituted for temperature, using an exponentially decreasing geothermal gradient with 300K at the surface and 1850K at 500 km depth. *From Ashby and Verrall, 1978.*

9.10.1 How to Construct a Deformation Mechanism Map

The concept of deformation mechanism maps is best understood and appreciated when you construct your own. In Table 9.5, therefore, we list constitutive equations for various deformation mechanisms in natural limestones and marbles, which will allow you to construct a deformation mechanism map.

TABLE 9.5 **EXPERIMENTALLY DERIVED CONSTITUTIVE EQUATIONS USED FOR THE CONSTRUCTION OF FIGURE 9.36**

Exponential-law creep:	$\dot{e} = 10^{5.8}\, e^{(-62{,}000/RT + \sigma/114)}$
Power-law creep regime *a:*	$\dot{e} = 10^{-5.5}\, e^{(-75{,}000/RT)}\, \sigma^{6.0}$
Power-law creep regime *b:*	$\dot{e} = 10^{3.8}\, e^{(-86{,}000/RT)}\, \sigma^{2.9}$
Superplastic creep:	$\dot{e} = 10^{5.0}\, e^{(-51{,}000/RT)}\, \sigma^{1.7}\, d^{-3}$

$\dot{e}$ = strain rate (s^{-1})
σ = differential stress (bar)
T = absolute temperature (K)
R = gas constant
d = grain size (μm)
Source: Rutter (1974), Schmid et al. (1977), Schmid (1982).

First, choose the axes of the plot. Let's decide to plot differential stress versus temperature. Now calculate the corresponding strain rate from each of the four constitutive equations at a specific stress and temperature condition (i.e., a point in the diagram). You recall that the mechanism producing the highest strain rate is dominant, so from the four solutions the one with the highest strain rate is dominant at that particular point in the diagram. Using individual points to fill the diagram is an unnecessarily slow and cumbersome approach. Instead, we calculate the stress–temperature curves at a given strain rate for each equation and plot these four curves in the diagram. Because some of these curves intersect, the final strain rate curve is composed of segments of the four curves for which the differential stress is smallest. When using different strain rates you will see that the positions of intersection points change. Also, the dominant deformation mechanism may change. Connecting these intersection point where mechanisms change defines the boundary between fields. A worked-out example is shown in Figure 9.37, in which differential stress is plotted as a function of grain size for T = 475°C. You can vary environmental conditions, such as stress, temperature, and grain size, and calculate the corresponding map using fairly simple spreadsheet calculations on a personal computer.

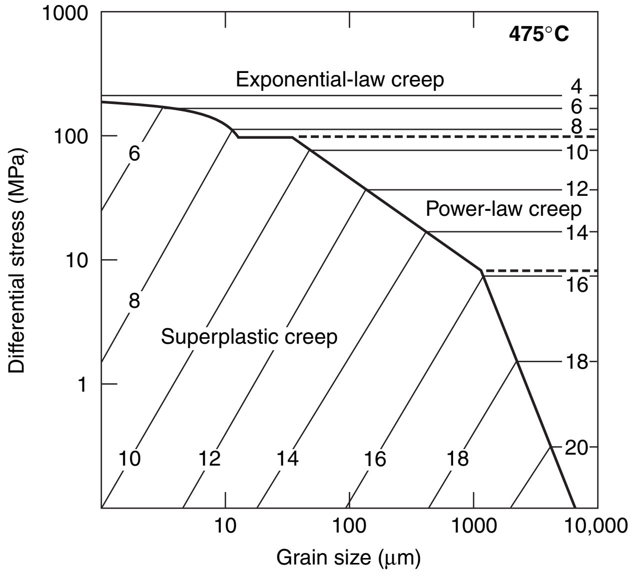

FIGURE 9.37 Deformation mechanism map for calcite at $T = 475$°C, constructed from the constitutive equations listed in Table 9.5. The thin lines represent strain rates (marked as –log), whereas the thick lines separate deformation mechanism fields.

9.10.2 A Note of Caution

Deformation mechanism maps evaluate all types of material behavior, which is not restricted to rocks. They also permit predictions of the creep of metal in a nuclear reactor, thereby aiding their safe design; they determine the lifespan of lightbulb filaments; they explain the creep of ice sheets; and they provide crucial information on the sagging rate of ancient marble benches in parks (Figure 9.38). So, deformation mechanism maps are a powerful approach to understanding and exploring the rheology of materials, and to applying this information to significant earth science problems such as mantle convection or lithosphere subduction. However, these maps are not without limitations. First, extrapolation over several orders of magnitude is needed to move from experimentally derived flow laws ($\dot{e} > 10^{-8}$/s) to geologic conditions ($\dot{e} < 10^{-11}$/s), introducing a major source of uncertainty. Second, the maps assume steady-state flow (i.e., that stress is strain-independent), which may not be sufficiently representative of geologic conditions. Moreover, evolving microstructures affect the dominant deformation mechanism; for example, dynamic recrystallization tends to reduce the grain size, which in turn enhances the importance of diffusional creep and weakens the material. In spite of these limitations, deformation mechanism maps are a handy and powerful tool to evaluate and predict deformation mechanisms and ambient conditions for deforming materials. Comparison of natural deformation structures with predictions based on deformation mechanism maps offers a natural test, which indeed indicates that these maps provide reliable estimates about the conditions of

FIGURE 9.38 Sharply dressed man with deformed marble bench that plastically sagged and locally fractured under the influence of gravity (and users).

TABLE 9.6 DEFORMATION MECHANISMS AND PROCESSES

Process (P) or Mechanism (M)	Atomic-Scale Process	Diagnostic Microstructures	Rheological Implications	Common Minerals
Bulk rotation (M or P)	Physical rotation of whole or part of mineral grains	Helical inclusion trails, bending of crystals, delta and sigma porphyroclasts		Any
Climb (M)	Diffusional addition or removal of atoms at dislocation line			Any; more at high T
Diffusive mass transfer (M or P)	"Long range" diffusion of atoms	Veins, pressure shadows, porphyroblasts		Any, especially quartz and calcite
Dislocation glide (M)	Rearrangement of interatomic bonds	Deformation lamellae, deformation bands, undulose extinction	$\dot{e} \propto \sigma^3$, also a hardening with finer grain size	Any; more at low stress and high T
Fracturing (M)	Breaking of interatomic bonds	Gouge, breccias, boudinaged grains		Any; more at high stress and low T
Frictional sliding (M)	Frictional sliding on surfaces	Gouges, breccias, pseudotachylytes, domino grains	$\tau \propto \sigma^n$	Any; more at high stress and low T
Grain boundary migration (P or M)	Local diffusion and reorientation of atoms or atomic clusters	Irregular grain boundaries, pinning microstructures, orientation families; lattice-preferred orientations with strong point maxima, non-120° triple junctions	Produces low dislocation density; material softer	Any; more at high T; especially quartz, olivine, feldpar
Grain boundary sliding (M)	Dislocation movement on "clean" grain boundaries, shearing on "dirty" ones			Any

(From Jessell and Bons, 2002)

deformation. Now return to Figures 9.34 to 9.36, showing deformation mechanism maps for several common minerals, and use them to think about the interplay between deformation mechanism, strain rate, temperature, and stress, and the associated microstructures. These maps also offer a useful way to absorb and appreciate the various mechanisms and processes of ductile deformation that were the focus of this chapter.

9.11 CLOSING REMARKS

Modern structural geology interpretations are relying increasingly on a synthesis of observations on all scales, including microscopic. An analysis of microstructures plays a growing role in unraveling the deformation histories of rocks and regions. For example, mechanical twinning can be used to unravel the early stress and strain history of fold-and-thrust belts; mylonitic microstructures allow us to estimate the conditions of T; σ_d, and $\dot{e}$ during deformation, and olivine fabrics in xenoliths, give us information on conditions of mantle flow. One additional consequence of crystal plastic deformation, crystallographic-preferred fabrics, will be introduced in Chapter 12. Meanwhile, we will explore common ductile structures in outcrop, namely folds, foliations, and lineations, in the next chapters. We close this chapter with a summary table (Table 9.6) that groups mechanisms and processes, and serves as a handy reference.

ADDITIONAL READING

Ashby, M. F., and Verrall, R. A., 1978. Micromechanisms of flow and fracture, and their relevance to

TABLE 9.6 (CONTINUED)

Process (P) or Mechanism (M)	Atomic-Scale Process	Diagnostic Microstructures	Rheological Implications	Common Minerals
Kinking (M)	Dislocation glide on single slip system	Kink bands		Micas, low *T* quartz, kyanite
Lattice diffusion (M)	Diffusional movement of vacancies and interstitials	New crystal void of preexisting impurities (hard to prove in nature)	$\dot{e} \propto \sigma/d^2$ (Nabarro-Herring creep); $\dot{e} \propto \sigma/d^3$ (Coble creep)	Any; more at low stress and high *T*
Lattice rotation (P)	Dislocation glide and/or bulk rotation of grains	Lattice-preferred orientations	Well-developed fabrics may be stronger or weaker than random fabrics	Any; more at low stress and high *T*
Phase change (M or P)	Changed crystal structure without change in bulk chemistry	Phase boundaries in minerals	Often associated with volume change	Quartz, calcite-aragonite, olivine
Recovery (P)	Climb, mutual annihilation of dislocations of opposite signs, formation of subgrain walls	Polygonization, foam texture, 120° triple junctions	Produces low dislocation density; material softer	Any; more at high *T*
Rotation recrystallization (P)	Progressive addition of dislocations of same sign to subgrain wall	Mortar texture or core-and-mantle texture, bimodal grain size	Change in grain size can strengthen or weaken material	Any; more at low stress and high *T*, especially quartz, feldspar, olivine
Twinning (M)	Rearrangement of interatomic bonds and reorientation of lattice site	Twins (sharp-nosed, narrow, parallel to rational twin planes)		Calcite (low *T* and low strain), plagioclase, quartz, amphibole

the rheology of the upper mantle. *Philosophical Transactions of the Royal Society of London,* Series A, 288, 59–95.

Frost, H. J., and Ashby, M. F., 1982. *Deformation-mechanism maps. The plasticity and creep of metals and ceramics.* Pergamon Press: Oxford.

Groshong, R. J., Jr., 1972. Strain calculated from twinning in calcite. *Geological Society of America Bulletin,* 83, 2025–2038.

Hayden, H. W., Moffatt, W. G., and Wulff, J., 1965. *The structure and properties of materials: Volume III, Mechanical behavior.* J. Wiley and Sons: New York.

Hull, D., and Bacon, D. J., 1984. *Introduction to dislocations.* Pergamon Press: Oxford.

Jamison, W. R., and Spang, J. H., 1976. Use of calcite twin lamellae to infer differential stress. *Geological Society of America Bulletin,* 87, 868–872.

Jessell, M., and Bons, P., 2002. *On-line short course in microstructures.* http://www.earth.monash.edu.au/Teaching/mscourse/index.html.

Loretto, M. H., and Smallman, R. E., 1975. *Defect analysis in electron microscopy.* Chapman and Hall: London.

Mercier, J.-C., Anderson, D. A., and Carter, N. L., 1977. Stress in the lithosphere: inferences from steady-state flow of rocks. *Pure and Applied Geophysics,* 115, 199–226.

Nicolas, A., and Poirier, J.-P., 1976. *Crystalline plasticity and solid state flow in metamorphic rocks.* John Wiley and Sons: London.

Ord, A., and Christie, J. M., 1984. Flow stresses from microstructures in mylonitic quartzites of the Moine thrust zone, Assynt area, Scotland. *Journal of Structural Geology,* 6, 639–654.

Poirier, J.-P., 1985. *Creep in crystals: high-temperature deformation processes in metals, ceramics and minerals.* Cambridge University Press: Cambridge.

Ross, J. V., Ave Lallemant, H. G., and Carter, N. L., 1980. Stress dependence of recrystallized-grain and subgrain size in olivine. *Tectonophysics,* 70, 39–61.

Rutter, E. H., 1974. The influence of temperature, strain rate and interstitial water in the experimental deformation of calcite rocks. *Tectonophysics,* 22, 311–334.

Schmid, S. M., Boland, J. N., and Paterson, M. S., 1977. Superplastic flow in finegrained limestone. *Tectonophysics,* 43, 257–291.

Schmid, S. M., Paterson, M. S., and Boland, J. N., 1980. High temperature flow and dynamic recrystallization in Carrara marble. *Tectonophysics,* 65, 245–280.

Spang, J. H., 1972. Numerical method for dynamic analysis of calcite twin lamellae. *Geological Society of America Bulletin,* 83, 467–472.

Turner, F. J., 1953. Nature and dynamic interpretation of deformation in calcite of three marbles. *American Journal of Science,* 251, 276–298.

Twiss, R. J., 1986. Variable sensitivity piezometric equations for dislocation density and subgrain diameter and their relevance to quartz and olivine. In Hobbs, B. E., and Heard, H. C., eds., *Mineral and rock deformation: laboratory studies (the Paterson volume),* American Geophysical Union, Geophysical Monograph 36, pp. 247–261.

Urai, J. L., Means, W. D., and Lister, G. S., 1986. Dynamic recrystallization of minerals. In Hobbs, B. E., and Heard, H. C., eds., *Mineral and rock deformation: laboratory studies (the Paterson volume*), American Geophysical Union, Geophysical Monograph 36, pp. 161–200.

Wenk, H.-R. (ed.), 1985. *Preferred orientation in deformed metals and rocks: an introduction to modern texture analysis.* Academic Press: Orlando.

White, S., 1976. The effects of strain on the microstructures, fabrics, and deformation mechanisms in quartzites. *Philosophical Transactions of the Royal Society of London,* Series A, 283, 69–86.

APPENDIX: DISLOCATION DECORATION

The principle behind optical imaging by dislocation decoration of olivine is that iron oxides preferentially precipitate along defects in olivine. In order to decorate dislocations in olivine, a sample with one polished surface is heated in air for approximately one hour at 900°C. A standard petrographic thin section is then prepared with the previously polished surface in contact with the glass slide. For most crystallographic directions, dislocation lines as far as 50 μm from the polished surface are decorated. Under the optical microscope, screw dislocations generally appear as long and straight lines. Using a microscope that is equipped with a universal stage, the crystallographic relationship can be determined. Decoration is most effective in samples with relatively low dislocation densities ($<10^8/\text{cm}^2$), such as mantle xenoliths in volcanic flows.